

# A Model of the Electrophysiological Properties of Thalamocortical Relay Neurons

DAVID A. McCORMICK AND JOHN R. HUGUENARD

*Section of Neurobiology, Yale University School of Medicine, New Haven, Connecticut 06510; and  
Department of Neurology, Stanford University Medical School, Stanford, California 94305*

## SUMMARY AND CONCLUSIONS

1. A model of the electrophysiological properties of single thalamocortical relay neurons in the rodent and cat dorsal lateral geniculate nucleus was constructed, based in part on the voltage dependence and kinetics of ionic currents detailed with voltage-clamp techniques. The model made the simplifying assumption of a single uniform compartment and incorporated a fast and transient  $\text{Na}^+$  current,  $I_{\text{Na}}$ ; a persistent, depolarization-activated  $\text{Na}^+$  current,  $I_{\text{Nap}}$ ; a low-threshold  $\text{Ca}^{2+}$  current,  $I_{\text{T}}$ ; a high-threshold  $\text{Ca}^{2+}$  current,  $I_{\text{L}}$ ; a  $\text{Ca}^{2+}$ -activated  $\text{K}^+$  current,  $I_{\text{C}}$ ; a transient and depolarization-activated  $\text{K}^+$  current,  $I_{\text{A}}$ ; a slowly inactivating and depolarization-activated  $\text{K}^+$  current,  $I_{\text{K2}}$ ; a hyperpolarization-activated cation current,  $I_{\text{h}}$ ; and  $\text{K}^+$  and  $\text{Na}^+$  leak currents  $I_{\text{Kleak}}$  and  $I_{\text{Naleak}}$ .

2. The effects of the various ionic currents on the electrophysiological properties of thalamocortical relay neurons were initially investigated through examining the effect of each current individually on passive membrane responses. The two leak currents,  $I_{\text{Kleak}}$  and  $I_{\text{Naleak}}$ , determined in large part the resting membrane potential and the apparent input resistance of the model neuron. Addition of  $I_{\text{A}}$  resulted in a delay in the response of the model cell to a depolarizing current pulse, whereas addition of  $I_{\text{K2}}$ , or  $I_{\text{L}}$  combined with  $I_{\text{C}}$ , resulted in a marked and prolonged decrease in the response to depolarization. Addition of  $I_{\text{h}}$  resulted in a depolarizing "sag" in response to hyperpolarization, whereas addition of  $I_{\text{T}}$  resulted in a large rebound  $\text{Ca}^{2+}$  spike after hyperpolarization. Finally, addition of  $I_{\text{Nap}}$  resulted in enhancement of depolarization.

3. The low-threshold  $\text{Ca}^{2+}$  spike of rodent neurons was successfully modeled with the active currents  $I_{\text{T}}$ ,  $I_{\text{L}}$ ,  $I_{\text{A}}$ ,  $I_{\text{C}}$ , and  $I_{\text{K2}}$ . The low-threshold  $\text{Ca}^{2+}$  current  $I_{\text{T}}$  generated the low-threshold  $\text{Ca}^{2+}$  spike. The transient  $\text{K}^+$  current  $I_{\text{A}}$  slowed the rate of rise and reduced the peak amplitude of the low-threshold  $\text{Ca}^{2+}$  spike, whereas the slowly inactivating  $\text{K}^+$  current  $I_{\text{K2}}$  contributed greatly to the repolarization of the  $\text{Ca}^{2+}$  spike. Activation of  $I_{\text{L}}$  during the peak of the  $\text{Ca}^{2+}$  spike led to activation of  $I_{\text{C}}$ , which also contributed to the repolarization of the  $\text{Ca}^{2+}$  spike. Reduction of any one of the  $\text{K}^+$  currents resulted in an increase in the other two, thereby resulting in substantially smaller changes in the  $\text{Ca}^{2+}$  spike than would be expected on the basis of the amplitude of each ionic current alone.

4. Activation of the various  $\text{K}^+$  currents,  $I_{\text{A}}$ ,  $I_{\text{K2}}$ , and  $I_{\text{C}}$ , also resulted in apparent rectification of the model neuron such that the response to a depolarizing current pulse was substantially smaller than the response to a hyperpolarizing current pulse.

5. Fast,  $\text{Na}^+$ -dependent action potentials were repolarized largely by  $I_{\text{C}}$  at membrane potentials positive to  $-60$  mV, with smaller contributions by  $I_{\text{A}}$  and  $I_{\text{K2}}$ . In contrast,  $I_{\text{A}}$  and  $I_{\text{K2}}$  formed a major component of the ionic currents flowing in between action potentials and therefore slowed the rate of action potential generation.

6. Addition of the hyperpolarization activated cation current  $I_{\text{h}}$  resulted in a depolarizing sag on hyperpolarization and generated an apparent afterhyperpolarization after a low-threshold  $\text{Ca}^{2+}$  spike. During the generation of a low-threshold  $\text{Ca}^{2+}$  spike,  $I_{\text{h}}$  deactivated, resulting in the membrane potential's falling to a more negative level on repolarization of the  $\text{Ca}^{2+}$  spike. Subsequent activation of  $I_{\text{h}}$  resulted in repolarization of the membrane potential and therefore the appearance of an afterhyperpolarization.

7. Rhythmic low-threshold  $\text{Ca}^{2+}$  spikes and burst generation were successfully modeled and depended critically on  $I_{\text{T}}$ ,  $I_{\text{h}}$ , and the leak currents  $I_{\text{Kleak}}$  and  $I_{\text{Naleak}}$ . The frequency and amplitude of rhythmic  $\text{Ca}^{2+}$  spike generation was strongly modulated by the amplitude of  $I_{\text{h}}$ ,  $I_{\text{T}}$ , and  $I_{\text{Kleak}}$ . Increasing the maximal conductance of  $g_{\text{h}}$  resulted in an increase in rhythmic burst generation from 0.5 to a maximum of 4 Hz. Shifting the voltage dependence of  $I_{\text{h}}$  by  $\pm 10$  mV resulted in an increase and decrease, respectively, of the frequency of rhythmic  $\text{Ca}^{2+}$  spike generation and a decrease and increase, respectively, of the ability of the cell to maintain rhythmic oscillation.

8. The response of the model to depolarizing inputs was markedly different during rhythmic oscillation than during tonic depolarization. During rhythmic oscillation, depolarization of the model cell resulted in a transient burst response and disruption of rhythmic burst discharges, whereas application of the same depolarizing current pulse in the tonic firing mode resulted in a train of action potentials that displayed no spike frequency adaptation.

9. In summary, the present model of thalamocortical relay cells suggests that the various  $\text{K}^+$  currents in these neurons contribute to the repolarization of not only  $\text{Na}^+$  but also low-threshold  $\text{Ca}^{2+}$  spikes, control the temporal characteristics of repetitive firing, and generate an apparent rectification of the neuron at resting membrane potentials. The ionic currents  $I_{\text{T}}$  and  $I_{\text{h}}$  are critically involved in rhythmic low-threshold  $\text{Ca}^{2+}$  spike generation, which also depends critically on the status of the various "leak" conductances that determine the membrane potential and apparent input resistance of the cell. These findings confirm and extend previous suggestions based on intracellular recordings of thalamocortical relay cells obtained in vivo and in vitro.

## INTRODUCTION

In the accompanying paper (Huguenard and McCormick 1992), we presented mathematical models of the voltage dependence and kinetics of several ionic currents present in rodent thalamocortical relay cells including the low-threshold  $\text{Ca}^{2+}$  current,  $I_{\text{T}}$ ; the hyperpolarization-activated cation current,  $I_{\text{h}}$ ; the transient, depolarization-activated  $\text{K}^+$  current,  $I_{\text{A}}$ ; and the slowly inactivating, depolarization-activated  $\text{K}^+$  current,  $I_{\text{K2}}$ . In this paper, we utilize these mathematical models, plus those developed by others

(French et al. 1990; Kay and Wong 1987; Yamada et al. 1989), in an attempt to model the basic electrophysiological properties of single thalamocortical relay neurons.

Rodent thalamocortical relay cells have the interesting property of being able to generate action potentials in either of two modes, both in vivo and in vitro: 1) single spike, or tonic, firing in which action potentials are generated one at a time in trains and 2) burst firing in which the cell generates a rebound high-frequency burst of action potentials after a brief hyperpolarization generated either by a hyperpolarizing current pulse or by an inhibitory postsynaptic potential. These unique electrophysiological features of individual thalamocortical relay neurons have been proposed to be critical to the appearance of rhythmic oscillations in intrathalamic and thalamocortical circuits (Deschênes et al. 1984; Jahnsen and Llinás 1984a,b; reviewed by Steriade and Deschênes 1984; Steriade and Llinás 1988). Indeed, recently it has been demonstrated that even individual thalamocortical relay cells in the feline thalamus can maintain rhythmic  $\text{Ca}^{2+}$  spike-mediated burst activity when isolated in vitro (McCormick and Prince 1987; McCormick and Pape 1990a; Soltesz et al. 1991). The generation of this slow (0.5–4 Hz) oscillation was proposed to be due largely to the interaction of two currents: the low-threshold  $\text{Ca}^{2+}$  current  $I_T$  and the hyperpolarization-activated cation current  $I_h$  (McCormick and Pape 1990a).

One test of the various hypotheses concerning the contribution of the various ionic currents present in thalamocortical relay cells to their electrophysiological properties is the success with which an accurate mathematical model of the properties of these different currents is able to reconstruct the electrophysiological behavior of the neuron. In addition, mathematical models of neurons are valuable, for they allow the plotting of the amplitude and time course of each of the different ionic currents during electrical activity in the model neuron, as well as the easy examination of the possible effects of the alteration in the amplitude or properties of each ionic current on the electrophysiological behavior of the neuron.

In this model we demonstrate that the various  $\text{K}^+$  currents present in thalamic relay cells are likely to contribute to the repolarization of both  $\text{Na}^+$  and low-threshold  $\text{Ca}^{2+}$ -mediated action potentials and control the frequency and time course of repetitive firing. In addition, this model confirms and extends the suggestion that rhythmic  $\text{Ca}^{2+}$  spike generation depends critically on the interaction of  $I_T$  and  $I_h$  as well as on the status of  $\text{K}^+$  currents active at rest.

## METHODS

This model of thalamocortical relay cells was based on the mathematical description of  $I_T$ ,  $I_A$ ,  $I_{K2}$ , and  $I_h$  presented in the accompanying paper (Huguenard and McCormick 1992). In addition to these currents, thalamocortical relay cells are also known to possess a fast and transient  $\text{Na}^+$  current, a persistent  $\text{Na}^+$  current, a  $\text{Ca}^{2+}$ -activated  $\text{K}^+$  current, and a high-threshold  $\text{Ca}^{2+}$  current (Coulter et al. 1989; Jahnsen and Llinás 1984a,b; McCormick, unpublished observations). The mathematical model of the fast  $\text{Na}^+$  current was based on whole cell voltage-clamp recording obtained from acutely dissociated cortical pyramidal cells (Huguenard et al. 1988) and is presented in the APPENDIX. The mathematical model of the persistent  $\text{Na}^+$  current was based on the data of French et al. (1990) obtained from hippocampal pyramidal cells;

the model of the  $\text{Ca}^{2+}$ -activated  $\text{K}^+$  current was that of Yamada et al. (1989), derived from bullfrog sympathetic ganglion cells; and the model of the high-threshold  $\text{Ca}^{2+}$  current  $I_L$  was that of Kay and Wong (1987), based on data obtained from hippocampal pyramidal cells. Although it is likely that there are differences between these ionic currents of hippocampal, cortical, and sympathetic ganglion cells and those of thalamocortical relay cells, the inclusion of these currents in the present model was necessary to increase the accuracy of the emulation of the current-clamp behavior of thalamocortical relay neurons.

This model is a "point" or single compartment model in which all of the membrane behaves in unison. Although this is an obvious gross simplification of the complicated morphology of thalamocortical relay neurons (e.g., see Bloomfield et al. 1987; Sherman and Koch 1986), it was considered necessary because the spatial distributions of the various ionic currents are not known. When they become available, these spatial data can be incorporated into future versions of this model. In addition, the success of this "point" model in replicating the basic electrophysiological properties of thalamocortical relay neurons suggests that the modeling of the complicated dendritic morphology of these cells is not essential to the modeling of some of their basic electrophysiological features. Second, the dynamics of  $\text{Ca}^{2+}$  buffering in thalamocortical relay neurons are not known. In this model, we assumed a single exponential decay of  $[\text{Ca}^{2+}]_i$  in the inner 100 nm of space just beneath the supposed membrane. The time constant of this decay was adjusted to replicate the duration of afterhyperpolarizations (~60 ms) that occur after the generation of a single action potential (Jahnsen and Llinás 1984a,b).

The total membrane area in this model was assumed to be 29,000  $\mu\text{m}^2$ , which is in the range of feline thalamocortical relay cells (Bloomfield et al. 1987). Given a specific membrane capacitance of 1  $\mu\text{F}/\text{cm}^2$ , this yields an input capacitance of 0.29 nF. This value is within the range of input capacitances for feline thalamocortical relay cells in slices in vitro as measured by the response to small hyperpolarizing current pulses (0.15–0.8 nF; McCormick, unpublished observations). The maximal conductances of the various ionic currents were estimated by scaling the normalized conductance (nS/pF) from the data obtained by whole cell recording in dissociated thalamocortical relay neurons to that used here (0.29 nF; Table 1). The maximal conductance of  $I_h$  (10–30 nS) was based on voltage-clamp data obtained in thalamocortical neurons maintained as a slice, in vitro (McCormick and Pape 1990a).

The temperature used in the present model was set to 35.5°C, because this is the temperature at which the intracellular recordings from thalamocortical relay cells maintained in slices were obtained (e.g., McCormick and Pape 1990a). The kinetics of all currents, except  $I_T$  where it has been directly measured, were assumed to have a  $Q_{10}$  of 3. The extracellular concentration of  $\text{Ca}^{2+}$  used in slice experiments was 2.0 mM and therefore was adopted here in an attempt to model results obtained from intracellular recordings in slices. In accordance with this change in  $[\text{Ca}^{2+}]_o$ , and the resultant changes in screening charge, the voltage dependence of activation and inactivation of  $I_T$  was adjusted so that the values used for  $V_{1/2}$  in the Boltzmann equation were -60.5 mV (activation) and -84 mV (inactivation).

Numeric solution of the differential equations representing the kinetics of the different ionic currents was achieved for this paper by use of the fourth-order Runge-Kutta method. The time step of simulation continually varied, depending on the rate of change of the various ionic gates. For these simulations, the total change in ionic gates was limited to <1% during any particular time step. For preliminary results, a one- or two-step Euler integration method was used and was found to yield similar or identical results to the Runge-Kutta method while greatly increasing the speed of simulation. The simulation program was written for use on an IBM AT-

TABLE 1. *Maximal conductances for isolated and model cells*

	Isolated cells 17.5 pF at 23.5°C		Normalized,			Intact cell 290 pF at 35.5°C		Model Cell
	Range	Average	Range	Average	$Q_{10}$	Range	Average	
$p_L$	0.10–2.54	0.90	0.005–0.145	0.051	3	5.9–157	56	80
$p_T$	0.09–0.75	0.33	0.005–0.043	0.019	3	6.5–52	23	40
	Maximum permeability, cm <sup>3</sup> /s		S/cm <sup>2</sup>		$Q_{10}$	Maximum permeability, cm <sup>3</sup> /s		Model Cell
	Range	Average	Range	Average		Range	Average	
$g_A$	18.7–82.6	41.2	0.0011–0.0047	0.0024	1.6	0.5–2.4	1.2	1
$g_{K2}$	10.7–64.9	36.8	0.0006–0.0037	0.0021	1.58	0.3–1.9	1.1	1
$g_{Na}$			0.010–0.022	0.011	1.5	4.6–10.2	5.1	9

style computer with or without math coprocessor and with some type of screen graphics capability (Hercules, CGA, EGA, or VGA).

Intracellular recordings from guinea pig and cat dorsal lateral geniculate nucleus (LGNd) neurons illustrated here were obtained with the *in vitro* slice technique during the performance of experiments for previously published studies (McCormick 1991, 1992a; McCormick and Pape 1990a).

## RESULTS

Guinea pig thalamocortical relay neurons *in vitro* possess an average resting membrane potential of about  $-63$  mV, a resting input resistance of 30–90 M $\Omega$ , and an average membrane time constant of  $\sim 14$  ms (Jahnsen and Llinás 1984a; McCormick and Prince 1987; McCormick and Pape 1990a). In this model of guinea pig thalamocortical relay neurons, the two leak conductances  $g_{Kleak}$  and  $g_{Naleak}$  were adjusted to 15 and 6 nS, respectively to give a resting membrane potential of  $-63$  mV and a resting input resistance of 48 M $\Omega$ . Injection of inward or outward current pulses in this situation resulted in passive membrane responses with a time constant of 14 ms (Fig. 1, *A* and *D*; – – –). Addition of each of the modeled active currents one at a time resulted in unique alterations in the response of the modeled cell to the current pulses (Fig. 1). Addition of  $I_A$  resulted in a small hyperpolarization of the cell because of tonic activation of the A-current at  $-63$  mV, resulting from the small “window” between activation and inactivation of this current (see Fig. 4; Huguenard and McCormick 1992). Depolarization of the neuron transiently activated  $I_A$ , resulting in a delay with which the membrane potential obtained its maximum value (Fig. 1*A*). In contrast, the response of the neuron to the hyperpolarizing current pulse was largely unaltered by  $I_A$ .

Addition of  $I_{K2}$  resulted in a substantial decrease in the response of the model to depolarization, whereas the response to hyperpolarization was unchanged. In addition, like  $I_A$ , a small amount of  $I_{K2}$  was active at rest and therefore resulted in a small hyperpolarization of the model cell. Addition of the high-threshold  $Ca^{2+}$  current  $I_L$  and the  $Ca^{2+}$ -activated  $K^+$  current  $I_C$  also resulted in a marked decrease in the response of the model to depolarization, whereas the response to hyperpolarization was unchanged. These results indicate that the presence of  $I_A$ ,  $I_{K2}$ , and  $I_C$  together in the model should result in marked apparent

rectification, with electrotonic responses to outward current injection being substantially smaller than to inward current injection of the same amplitude.

Addition of the hyperpolarization-activated cation current  $I_h$  resulted in a small depolarization of the cell at rest because of a slight activation of this current at  $-63$  mV. The main effect of  $I_h$  was to generate a depolarizing sag in the response to the hyperpolarizing current pulse, whereas the response to the depolarizing current pulses was unchanged (Fig. 1*D*).

Turning on of the low-threshold  $Ca^{2+}$  current  $I_T$  resulted in the appearance of a rebound  $Ca^{2+}$  spike on offset of hyperpolarization (Fig. 1*E*). Interestingly, this rebound  $Ca^{2+}$  spike was associated with a large depolarization that peaked at 0 mV and repolarized as  $I_T$  inactivated. The large amplitude of the low-threshold  $Ca^{2+}$  spike in this simulation is due to the lack of active  $K^+$  currents (see below). The persistent  $Na^+$  current,  $I_{Nap}$ , resulted in an enhancement of the response to depolarizing current pulses, whereas the response to hyperpolarizing current pulses was only slightly enhanced. The persistence of the depolarization after the end of the outward current pulse in the present simulation indicates that plateau depolarizations would be produced by persistent  $Na^+$  currents in the absence of active  $K^+$  conductances.

### *Two modes of action potential generation*

Thalamocortical relay neurons *in vivo* or *in vitro* display two prominent modes of action potential generation: burst firing, in which two to six action potentials occur in a high-frequency (250–400 Hz) burst riding on a low-threshold  $Ca^{2+}$  spike; and single spike activity, in which action potentials are generated in trains, the frequency of which depends on the strength of depolarization (Deschênes et al. 1984; Jahnsen and Llinás 1984a). Burst firing in nonoscillating relay neurons is typically evoked by the offset of a hyperpolarizing current pulse and is often generated in response to an inhibitory postsynaptic potential *in vivo* (see Steriade and Deschênes 1984).

The present model of a guinea pig LGNd relay cell also exhibited these two modes of action potential generation. Injection of a hyperpolarizing current pulse at rest ( $-65$  mV) was followed by the generation of a rebound burst of

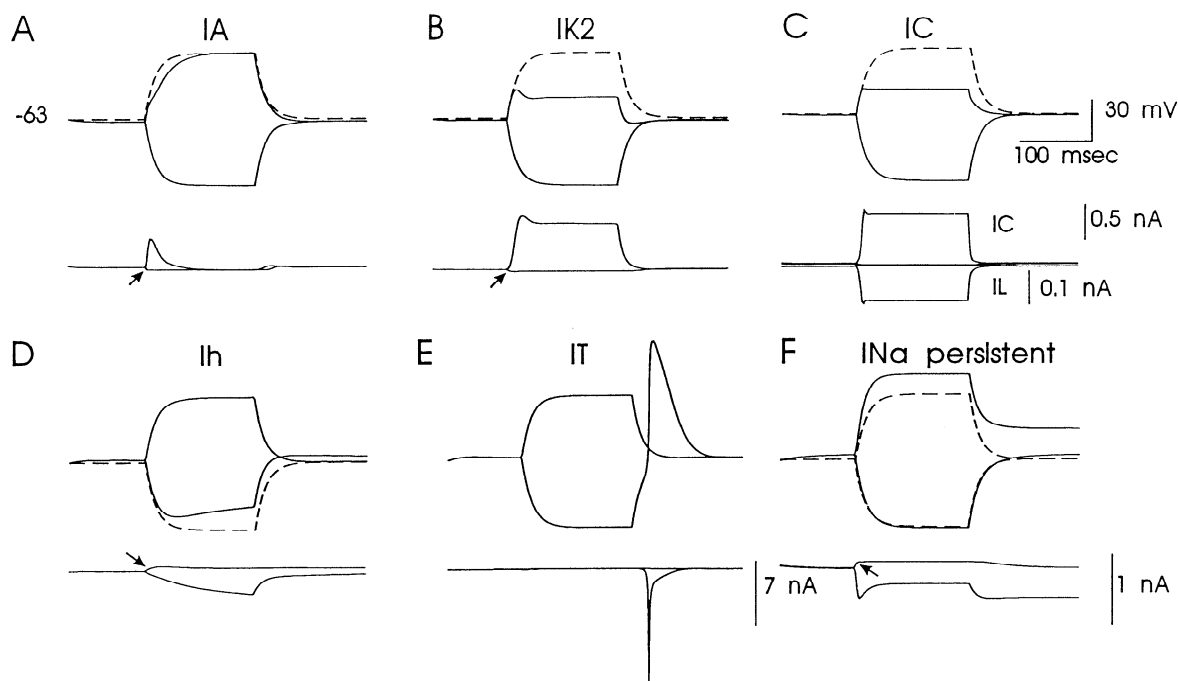


FIG. 1. Effect of addition of each current on the response of the model thalamic cell to an inward and outward current pulse of 1 nA. Model was initially set with an  $I_{Kleak}$  of 15 nS and an  $I_{Naleak}$  of 6 nS for a resting membrane potential of  $-63$  mV and an input impedance of  $48$  M $\Omega$ . *A*: addition of  $I_A$  results in a slowing of the rate of rise to the initial portion of the depolarizing current pulse (— is with  $0.8$   $\mu$ S  $I_A$ , --- is  $I_{Kleak}$  and  $I_{Naleak}$  only). Plot of the A-current (below the voltage trace) reveals that a small amount of  $I_A$  was active at rest ( $\nearrow$ ) because of a “window” current and thereby hyperpolarizing the cell by  $\sim 2$  mV. Depolarization of the cell results in activation followed by complete inactivation of  $I_A$ . Hyperpolarization of the cell results in removal of activation of  $I_A$ . *B*: addition of  $I_{K2}$  ( $0.8$   $\mu$ S) results in a substantial decrease in the response of the cell to the depolarizing current pulse. *C*: addition of the  $Ca^{2+}$  current  $I_L$  ( $80 \times 10^{-6}$  cm $^3$ /s) and the  $Ca^{2+}$ -activated current  $I_C$  ( $1$   $\mu$ S) results in a marked reduction in the response to depolarizing current pulses from the activation of  $I_L$  and the subsequent activation of  $I_C$  (bottom traces). *D*: addition of  $I_h$  ( $20$  nS) results in a time-dependent “sag” of the membrane potential in the hyperpolarizing range. Note small amount of  $I_h$  active at rest ( $\searrow$ ). *E*: addition of  $I_T$  ( $40 \times 10^{-6}$  cm $^3$ /sec) results in a rebound low-threshold  $Ca^{2+}$  spike that peaks at  $\sim 0$  mV. *F*: addition of  $I_{Na}$  persistent results in a marked increase in response to depolarizing current pulses. Depolarization persists because of the lack of K-currents to repolarize the cell.

four action potentials (Fig. 2*A*). The rebound burst resulted from the activation of the low-threshold  $Ca^{2+}$  current  $I_T$  (Fig. 2*A*,  $\nearrow$ ), whereas the fast action potentials were generated by the fast  $Na^+$  current  $I_{Na}$ . Thus hyperpolarization of the neuron with the current pulse led to removal of inactivation of  $I_T$ . On release of the hyperpolarizing current pulse, the membrane repolarized back toward rest, thereby activating  $I_T$  and subsequently generating a low-threshold  $Ca^{2+}$  spike. The low-threshold  $Ca^{2+}$  current then depolarized the neuron past the threshold for the generation of fast,  $Na^+$ -dependent action potentials.

Simulation of a depolarizing current pulse resulted in a train of four action potentials that showed little spike frequency adaptation, as in normal rodent and cat LGNd relay neurons (Jahnsen and Llinás 1984a,b; McCormick 1992a). In contrast to the hyperpolarizing current pulse, the depolarizing current pulse activated very little  $I_T$ , because of the nearly complete inactivation of this current at  $-65$  mV.

Therefore the model successfully replicated the presence of two basic modes of action potential generation in thalamocortical relay cells. Now we would like to consider in more detail the role of each of the different ionic currents in the generation of these two modes of electroresponsiveness.

#### Model of the low-threshold $Ca^{2+}$ spike

The low-threshold  $Ca^{2+}$  spike in rodent thalamocortical relay neurons was recorded in vitro after the block of voltage-dependent  $Na^+$  currents with the local application of tetrodotoxin ( $10$   $\mu$ M in micropipette) and after block of the hyperpolarization-activated cation current  $I_h$  with local application of  $Cs^+$  ( $20$  mM in micropipette; McCormick and Pape 1990a; Fig. 3*A*). Intracellular injection of a depolarizing current pulse while tonically hyperpolarizing the cell to  $-115$  mV to remove inactivation of  $I_T$  resulted in the elicitation of a low-threshold  $Ca^{2+}$  spike that was characterized by a rapid rate of rise, a much slower rate of fall, and the appearance of a fast “spike” and negative going “notch” at the peak of the  $Ca^{2+}$  spike (Fig. 3*A*,  $\checkmark$ ). Differentiation of the voltage trace with respect to time revealed that the rate of rise for this particular cell peaked at  $\sim 12$  V/s and that the rate of fall displayed both a fast and a slow phase (Fig. 3*A*,  $dV/dt$ ). The results of modeling of a guinea pig LGNd cell under the same conditions as that of the cell of Fig. 3*A* are illustrated in Fig. 3*B*. The model cell was held to  $-115$  mV and a current pulse of  $0.25$  nA was injected. The model cell generated a low-threshold  $Ca^{2+}$  spike, which exhibited a fast rate of rise and a fast and slow rate of fall (Fig. 3*B*) and

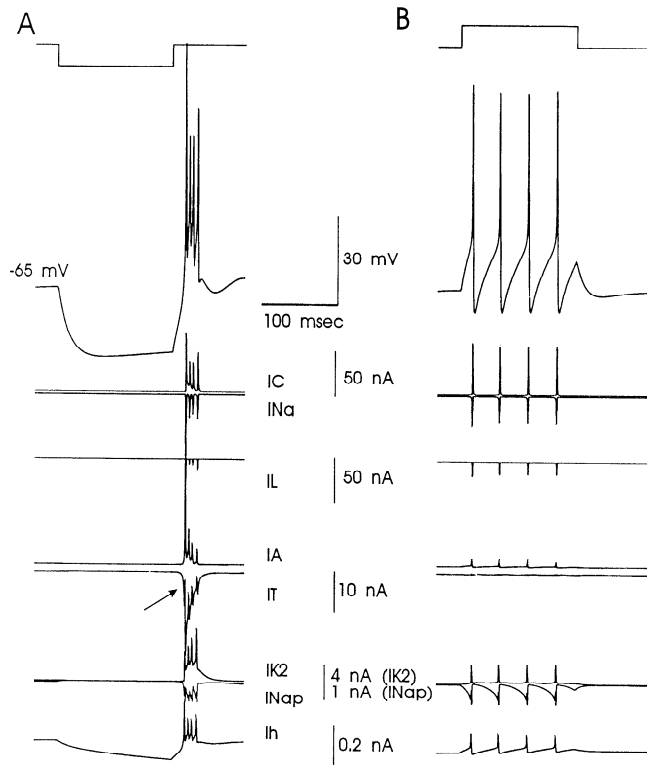


FIG. 2. Response of the model cell to hyperpolarizing and depolarizing current pulses. Hyperpolarizing current pulse is followed by a rebound burst of action potentials due to the activation of  $I_T$  ( $\nearrow$ ). Depolarizing current pulse results in a train of action potentials that displays little spike frequency adaptation and very little activation of  $I_T$  (as in real LGNd relay neurons).

the presence of a "peak" followed by a "notch" on the falling phase (Fig. 3B,  $\surd$ ). Although the peak rate of rise of the modeled  $\text{Ca}^{2+}$  spike (14 V/s) was higher than that in the cell in Fig. 3A, it is within the range reported for guinea pig thalamocortical relay cells (Jahnsen and Llinás 1984a).

The contribution of the different ionic currents contained in this model to the generation of the low-threshold  $\text{Ca}^{2+}$  spike was examined in more detail. At resting membrane potential of  $-63$  mV, and after block of  $I_{\text{Na}}$  and  $I_{\text{Nap}}$ ,

injection of a hyperpolarizing current pulse was followed by the occurrence of a rebound  $\text{Ca}^{2+}$  spike (Fig. 4A). A plot of the different ionic currents flowing during the rebound  $\text{Ca}^{2+}$  spike revealed that the  $\text{Ca}^{2+}$  spike was generated largely by the low-threshold  $\text{Ca}^{2+}$  current  $I_T$  with a small contribution by the high-threshold  $\text{Ca}^{2+}$  current  $I_L$  (Fig. 4, A and C). A plot of the different potassium currents during the generation of the  $\text{Ca}^{2+}$  spike revealed that  $I_A$ ,  $I_C$ , and  $I_{K2}$  all contributed to this electrophysiological response (Fig. 4, A and C). The A-current activated earlier and more rapidly than  $I_C$  or  $I_{K2}$  and therefore contributed substantially to the rising phase of the  $\text{Ca}^{2+}$  spike (Fig. 4C). After the  $\text{Ca}^{2+}$  spike reached approximately  $-45$  mV,  $I_L$  became increasingly active, thereby activating  $I_C$  at about the peak of the  $\text{Ca}^{2+}$  spike. This activation of  $I_C$  is in large part responsible for the "notch" on the initial repolarizing phase of the  $\text{Ca}^{2+}$  spike. The slowly inactivating  $\text{K}^+$  current  $I_{K2}$  was active throughout the repolarization of the  $\text{Ca}^{2+}$  spike and became the dominant  $\text{K}^+$  current approximately halfway through repolarization (Fig. 4C). Therefore all three  $\text{K}^+$  currents appear to be involved in the shaping of the amplitude-time course of low-threshold  $\text{Ca}^{2+}$  spikes, with  $I_A$  dominant during the rise of the  $\text{Ca}^{2+}$  spike,  $I_C$  dominant during the initial phases of repolarization, and  $I_{K2}$  dominant during the remainder of repolarization (Fig. 4C).

To test this hypothesis, each of the different  $\text{K}^+$  currents was reduced or blocked individually and in combination to examine the subsequent effect on the low-threshold  $\text{Ca}^{2+}$  spike. In addition to revealing the role of each of the different  $\text{K}^+$  currents in the shaping of the low-threshold  $\text{Ca}^{2+}$  spike, these simulations also revealed the interesting finding that reduction of any one of the  $\text{K}^+$  currents results in a compensatory increase in the other two, thereby resulting in smaller changes in the amplitude-time course of the  $\text{Ca}^{2+}$  spike than might be expected given the plots of the amplitude-time course of the different currents in Fig. 4C (see also Yamada et al. 1989).

Reduction of  $I_A$  resulted in a substantial increase in the rate of rise of the low-threshold  $\text{Ca}^{2+}$  spike and an increase in its peak amplitude (Fig. 4A), with little effect on its duration (not shown). Reduction or block of  $I_C$  resulted in a loss

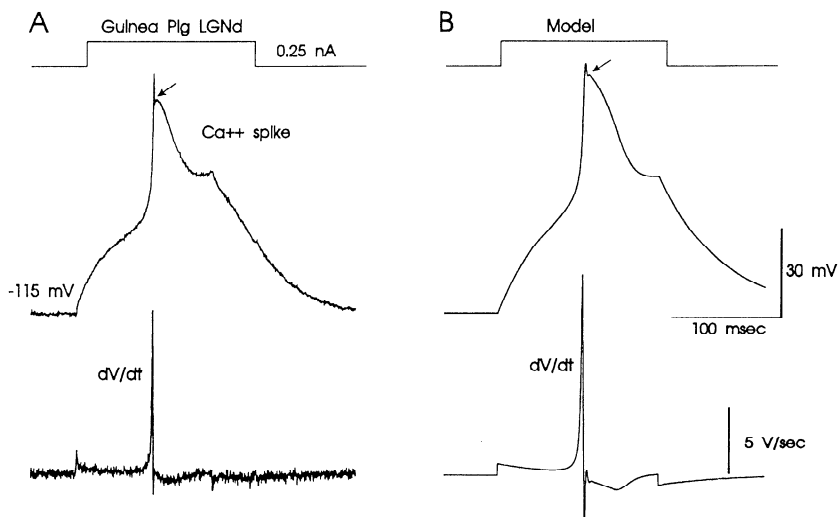


FIG. 3. Simulation of low-threshold  $\text{Ca}^{2+}$  spikes in guinea pig LGNd relay neurons. A: injection of a 0.25-nA current pulse in a guinea pig LGNd relay cell after the block of  $\text{Na}^+$  conductances with tetrodotoxin (TTX; 10  $\mu\text{M}$  in micropipette) and  $I_h$  with external  $\text{Cs}^+$  (20 mM in micropipette) and while holding the cell to  $-115$  mV to remove inactivation of  $I_T$ . Low-threshold  $\text{Ca}^{2+}$  spike is characterized by the presence of a marked "notch" in the initial parts of repolarization ( $\surd$ ). Differentiation of the voltage trace with respect to time ( $dV/dt$ ) is plotted below. B: model of a guinea pig LGNd neuron. Again the low threshold  $\text{Ca}^{2+}$  spike displays a prominent "notch" during repolarization.

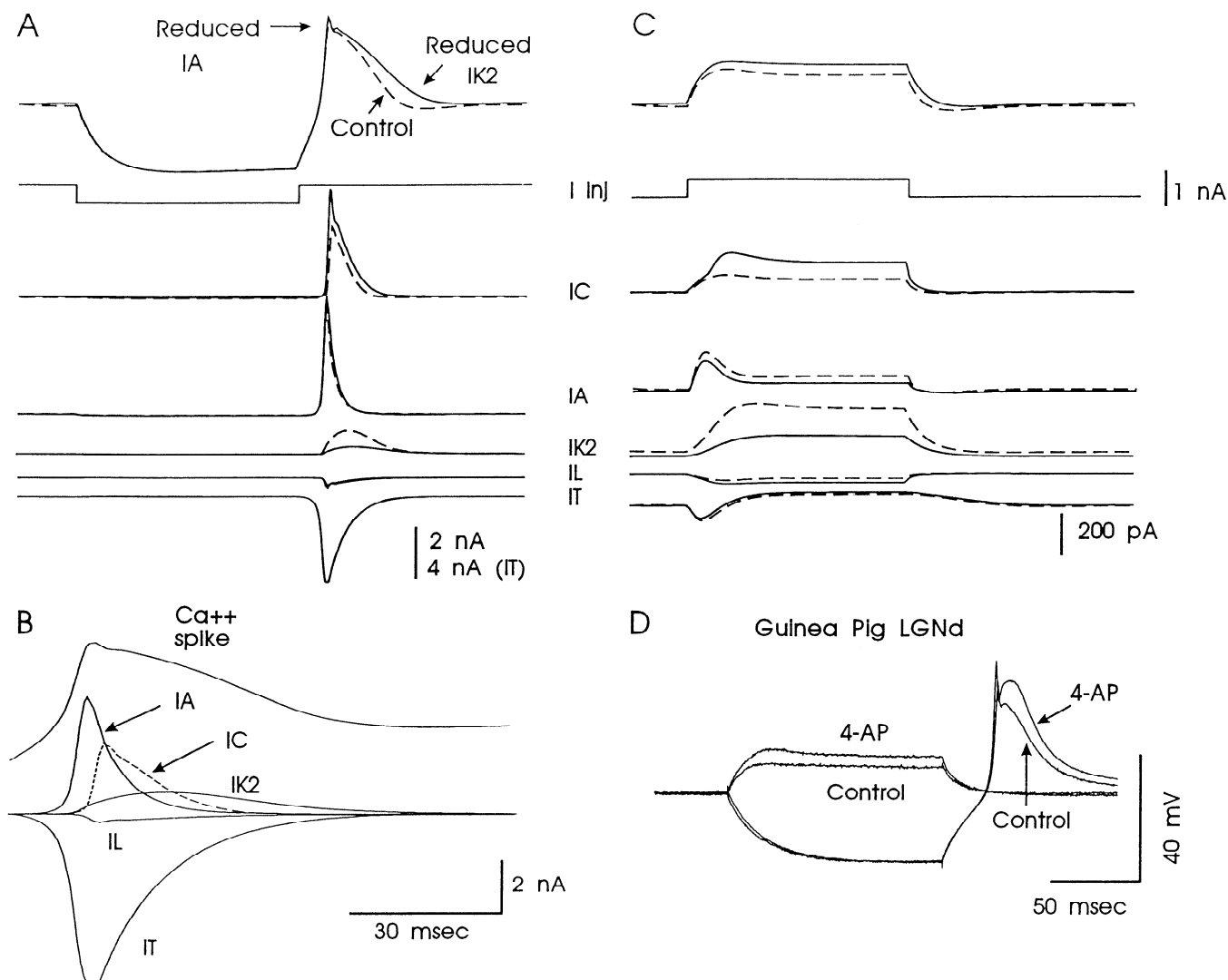


FIG. 4. Amplitude-time course of different currents during injection of hyperpolarizing and depolarizing current pulses in a model guinea pig LGNd relay cell without active  $\text{Na}^+$  conductances. *A*: injection of a hyperpolarizing current pulse results in a rebound  $\text{Ca}^{2+}$  spike (---). Plot of different currents illustrates that the  $\text{Ca}^{2+}$  spike is generated by  $I_T$  with a small contribution of  $I_L$  and is repolarized by inactivation of  $I_T$  and activation of the various  $\text{K}^+$  currents,  $I_C$ ,  $I_A$ , and  $I_{K2}$ . Reduction of  $I_{K2}$  from 0.8 to 0.2  $\mu\text{S}$  results in a substantial broadening of the duration of the  $\text{Ca}^{2+}$  spike, whereas reduction of  $I_A$  from 0.8 to 0.6  $\mu\text{S}$  results in an increase in the rate of rise and peak amplitude of the  $\text{Ca}^{2+}$  spike (---, control; —, reduced  $I_{K2}$  and  $I_A$ ). Interestingly, resulting changes in the  $\text{Ca}^{2+}$  spike are smaller than might be suspected because of increased activation of  $I_C$ , which compensates in part for the reduced amplitude of  $I_{K2}$  and  $I_A$ . *B*: expanded plot of the low threshold  $\text{Ca}^{2+}$  spike and the amplitude-time course of the various currents. *C*: injection of a depolarizing current pulse of an amplitude equal to the hyperpolarizing current pulse results in marked apparent rectification because of the activation of the  $\text{K}^+$  currents (---). Reducing  $I_{K2}$  and  $I_A$  results in an increase in response to the depolarizing current pulse (—), although, again, there is a compensatory increase in  $I_C$  because of the increased depolarization (compare --- and —). *D*: response of a guinea pig LGNd cell to a hyperpolarizing and depolarizing current pulse before (control) and after addition of 4-AP (100  $\mu\text{M}$ ). This concentration of 4-AP should largely block the slowly inactivating  $\text{K}^+$  current  $I_{A2}$  (see McCormick 1991), with minor effects on the quickly inactivating  $\text{K}^+$  current  $I_A$  (see Huguenard et al. 1991). Note that the cell exhibits apparent rectification to the depolarizing current pulse, which is lessened with 4-AP, whereas the rebound  $\text{Ca}^{2+}$  spike is significantly increased in amplitude and duration by addition of this drug. Time base in *D* for *A*, *C*, and *D*.

of the hyperpolarizing “notch” in the low-threshold  $\text{Ca}^{2+}$  spike, an increase in the peak amplitude of this spike, an increase in activation of  $I_A$  and  $I_{K2}$ , and a subsequent decrease in the duration of the  $\text{Ca}^{2+}$  spike because of increased activation of  $I_{K2}$  (not shown). Reductions of  $I_{K2}$  resulted in substantial increases in the duration of the low-threshold  $\text{Ca}^{2+}$  spike and an increase in the amplitude of  $I_C$  (Fig. 4*A*). Reduction of  $I_A$  and  $I_{K2}$  together resulted in an

increase in the initial peak amplitude and duration of the  $\text{Ca}^{2+}$  spike (Fig. 4*A*). These results are similar to those obtained with intracellular recordings from guinea pig LGNd relay neurons in vitro (Fig. 4*D*). Here, application of 100  $\mu\text{M}$  4-aminopyridine (4-AP) results in a substantial increase in the duration of the low-threshold  $\text{Ca}^{2+}$  spike as well as an increase in its peak amplitude (Fig. 4*D*; McCormick 1991). Bath application of 100  $\mu\text{M}$  4-AP is known to

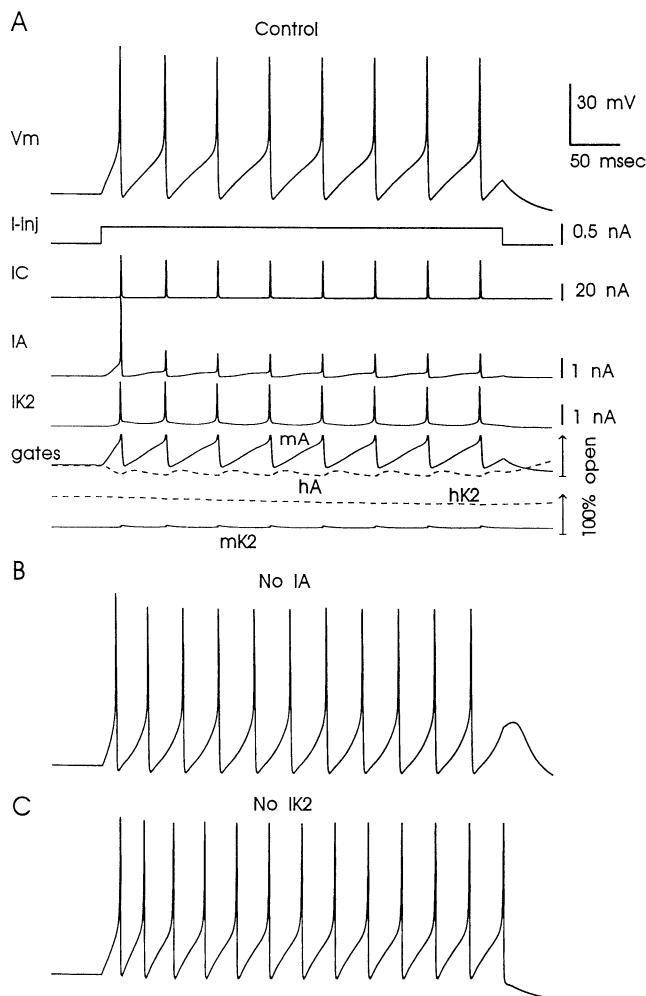


FIG. 5. Role of  $I_A$  and  $I_{K2}$  in control of repetitive firing in model relay neuron. *A*: injection of a depolarizing current pulse of 0.4 nA results in a train of action potentials. Amplitude-time course of 3 potassium currents ( $I_C$ ,  $I_A$ ,  $I_{K2}$ ) and the state of the activation ( $m_A$ ,  $m_{K2}$ ) and inactivation ( $h_A$ ,  $h_{K2}$ , ---) gates are shown. *B*: reduction of  $I_A$  to 0 results in a decrease in the interspike interval and an increase in the response of the cell to the depolarizing current pulse. *C*: similarly, block of  $I_{K2}$  also results in a decrease in the interspike interval.

block at least the slowly inactivating  $K^+$  current  $I_{A5}$ , a current that is electrophysiologically similar to  $I_{K2}$  (McCormick 1991).

Thalamocortical relay neurons in the rodent or cat LGNd display marked apparent rectification in that the response to a depolarizing current pulse is substantially smaller than that to an equal amplitude hyperpolarizing pulse (Fig. 4*D*, control). This rectification results in part from the activation of slowly inactivating  $K^+$  currents such as  $I_{A5}$  (McCormick 1991). Similarly, in the model, the cell displayed apparent rectification against depolarizing current pulses (compare Fig. 4, *A* and *B*). Plots of the different  $K^+$  currents indicated that  $I_{K2}$ ,  $I_A$ , and  $I_C$  were all activated by the depolarizing current pulse, resulting in a decrease in the amplitude of the subsequent depolarization (Fig. 4*B*). Reduction of  $I_{K2}$  from 0.8 to 0.2  $\mu$ S and  $I_A$  from 0.8 to 0.6  $\mu$ S resulted in an increase in the depolarizing response, although this increase was limited to only  $\sim 3$  mV, owing to compensatory increases in the amplitude of

$I_C$  (Fig. 4*B*, compare --- with —). Similar results have been obtained in guinea pig LGNd cells. Here, block of slowly inactivating  $K^+$  currents with 4-AP results in an increase in the amplitude of the response to a depolarizing current pulse with no change in the response to an equal amplitude hyperpolarizing current pulse (Fig. 4*D*; McCormick 1991).

#### Role of $I_A$ and $I_{K2}$ in repetitive firing

The role of the transient  $K^+$  currents  $I_A$  and  $I_{K2}$  in repetitive single spike activity was investigated by examining the amplitude-time course of these currents during the generation of trains of action potentials and the effect of block of these currents on the rate of action potential generation. Application of a depolarizing current pulse into the model cell resulted in a train of action potentials that showed only a small amount of spike frequency adaptation, as in real thalamocortical relay cells (McCormick 1992a). Plots of the different  $K^+$  currents revealed that although  $I_A$  and  $I_{K2}$  contributed to the repolarization of each  $Na^+$  action potential, the main  $K^+$  current involved in this was  $I_C$  (Fig. 5*A*). In contrast,  $I_A$  and  $I_{K2}$  formed the dominant  $K^+$  currents in between action potentials. In particular, the slow depolarization of the membrane potential toward the initiation of each  $Na^+$  action potential resulted in an increase in activation of  $I_A$  (Fig. 5*A*), which subsequently slowed the rate of depolarization and controlled the membrane potential trajectory as action potential threshold was approached. The occurrence of the action potential then rapidly activated  $I_A$  and failed to completely inactivate  $I_A$ ; therefore this current contributed to repolarization of the fast spike. Examination of the gates for  $I_A$  and  $I_{K2}$  indicated that the activation ( $m_A$ ) and inactivation ( $h_A$ ) variables for  $I_A$  were substantially more dynamic than the activation ( $m_{K2}$ ) and inactivation variables ( $h_{K2}$ ) for  $I_{K2}$  (Fig. 5*A*). This result indicates that variations in the amplitude of  $I_A$  are both the consequence of changes in the gates for  $I_A$  and the difference between the membrane potential and  $E_K$ , whereas variations in the amplitude of  $I_{K2}$  during a train of action potentials depend substantially on the driving force on  $K^+$  ions (Fig. 5*A*).

Reduction of either  $I_A$  or  $I_{K2}$  resulted in substantial increases in the firing frequency during the depolarizing current pulse (Fig. 5, *B* and *C*), confirming the importance of these ionic currents in the shaping of the train of action potentials. The rapidly inactivating  $K^+$  current  $I_A$  is dynamically involved in the shaping of each action potential after-hyperpolarization, whereas the kinetically slower current  $I_{K2}$  modulates firing rate through more prolonged changes in excitability.

#### Electrophysiological consequences of $I_h$

Rodent and cat LGNd cells in vivo and in vitro display a marked depolarizing "sag" upon hyperpolarization because of the activation of a hyperpolarization-activated cation current known as  $I_h$  (Fig. 6*A*; McCormick and Pape 1990a; Steriade et al. 1991). Similarly, addition of  $I_h$  to the model cell resulted in substantial depolarizing "sags" in the response to prolonged hyperpolarizations (Fig. 6*D*), owing to the activation of  $I_h$  (Fig. 6*E*). The amplitude and rate of

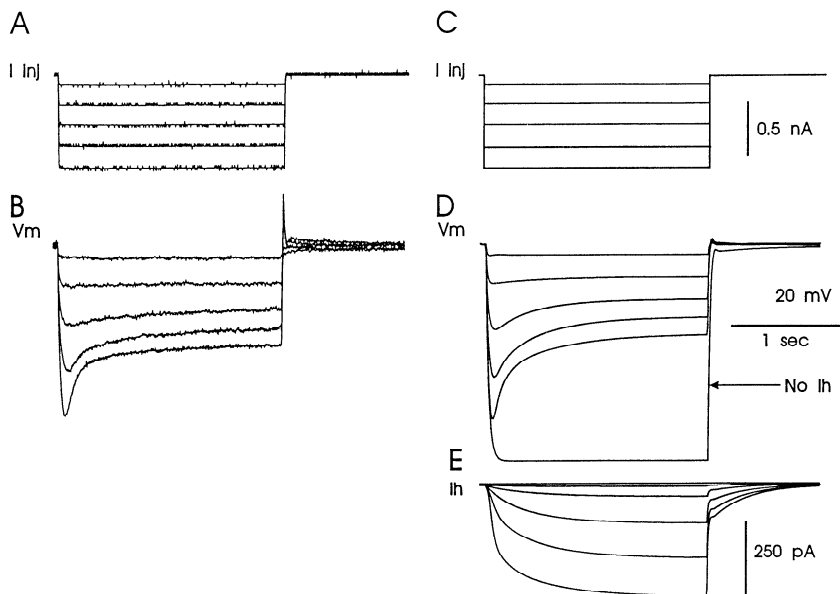


FIG. 6. Hyperpolarization-activated cation current  $I_h$  generates a substantial inward "sag" in the membrane response. *A* and *B*: intracellular responses of a guinea pig LGNd cell to prolonged (2 sec) hyperpolarizing current pulses after block of active  $\text{Na}^+$  current with TTX. Note the prominent inward sag in the hyperpolarizing direction. This sag is completely blocked by block of  $I_h$  with external  $\text{Cs}^+$  (not shown; McCormick and Pape 1990a). *C* and *D*: response of the model neuron to a prolonged hyperpolarizing current pulse. Activation of  $I_h$  (*E*) results in a marked depolarizing sag of the membrane potential (*D*). Block of  $I_h$  illustrates the response of the cell to the largest current pulse without this current (No  $I_h$ ).

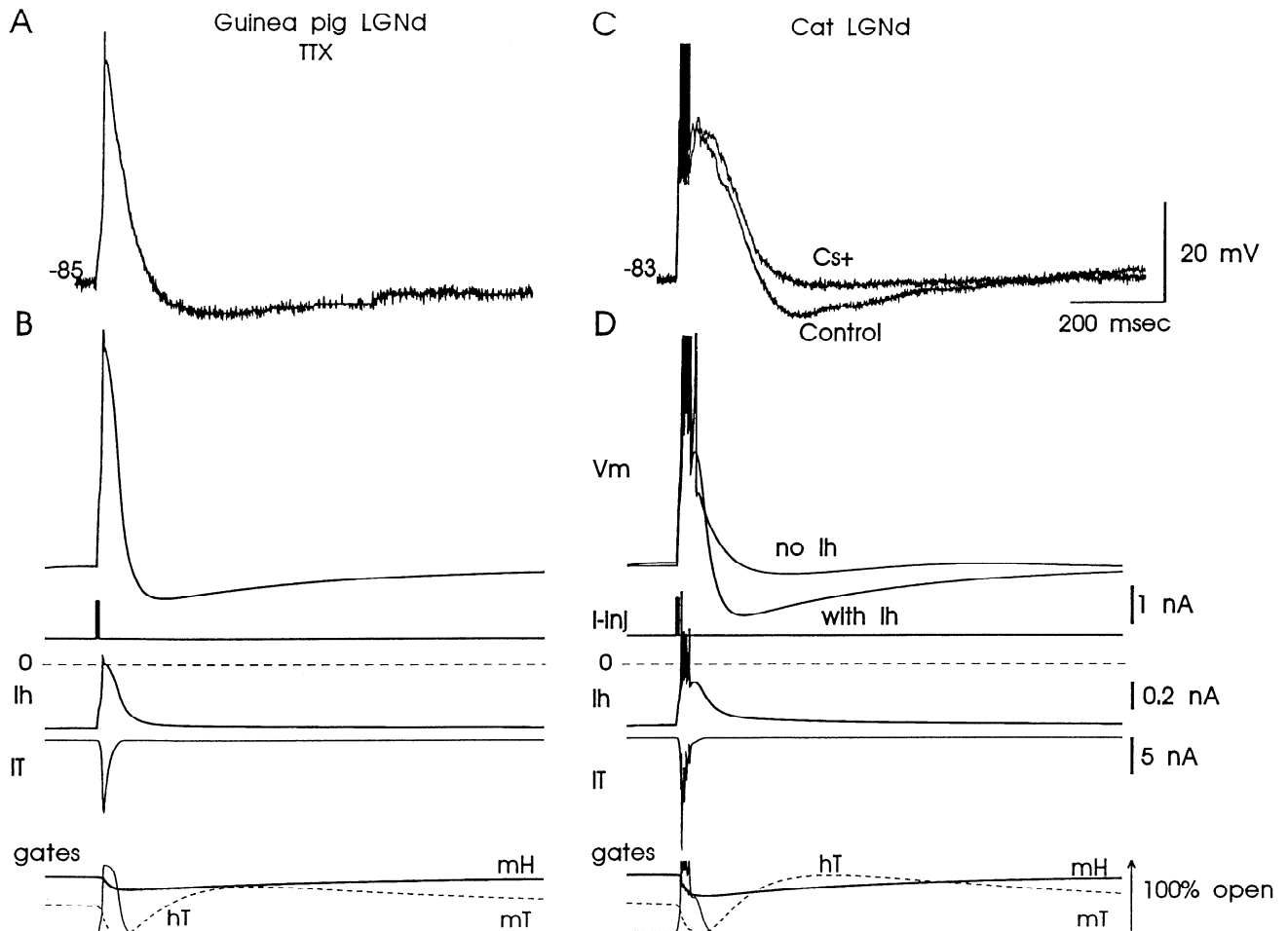


FIG. 7. Activation and deactivation of the H-current generates a slow afterhyperpolarization after a  $\text{Ca}^{2+}$  spike in guinea pig (*A*) and cat (*C*) LGNd cells. *A*: injection of a short-duration (10 msec) depolarizing current pulse into a guinea pig LGNd cell in the presence of TTX and after hyperpolarization to  $-85$  mV results in a low threshold  $\text{Ca}^{2+}$  spike, followed by an afterhyperpolarization. *B*: injection of a depolarizing current pulse in the model cell also results in a prolonged afterhyperpolarization, which is due to the activation of  $I_h$  (see  $I_h$  and  $m_h$ ). *C*: Activation of a low threshold  $\text{Ca}^{2+}$  spike in a cat LGNd cell results in a burst of  $\text{Na}^+$  spikes and a prolonged afterhyperpolarization. This afterhyperpolarization is almost completely blocked by reduction of  $I_h$  with extracellular application of  $\text{Cs}^+$  (10 mM in micropipette). Note the difference in duration of low threshold  $\text{Ca}^{2+}$  spikes in cat vs. guinea pig LGNd relay cells. *D*: model of the results in *C*. Block of  $I_h$  results in a nearly complete abolition of the slow afterhyperpolarization. Residual AHP is due to activation of  $I_{K2}$  (not shown).

repolarization of the membrane increased with increases in hyperpolarization of the modeled cell, owing to the decrease in time constant of activation of  $I_h$  and the increased activation of this current (see Fig. 7 in Huguenard and McCormick 1992). Block of  $I_h$  completely removed this electrophysiological feature of the model cell (Fig. 6D).

In cat LGNd cells it has been proposed that decreased activation and subsequent reactivation of  $I_h$  may form the slow afterhyperpolarization (AHP) that appears after the generation of a low-threshold  $\text{Ca}^{2+}$  spike (McCormick and Pape 1990a). Indeed, modeling of the generation of low-threshold  $\text{Ca}^{2+}$  spikes from a hyperpolarized membrane potential ( $-85$  mV) resulted in the appearance of a slow AHP, as in guinea pig LGNd cells in vitro (Fig. 7, A and B). Examination of the flow of ionic currents during the slow AHP in the model cell revealed that it is largely due to decreased activation ( $m_h$ ) of  $I_h$  during the  $\text{Ca}^{2+}$  spike and the subsequent reactivation of the current on repolarization (Fig. 7B). The residual AHP is due to activation of  $I_{K2}$  by the low-threshold  $\text{Ca}^{2+}$  spike (not shown).

Intracellular recordings from LGNd relay cells in guinea pig, rat, and cat have revealed that low-threshold  $\text{Ca}^{2+}$  spikes in cat are substantially longer in duration than those either in guinea pig or rat (Crunelli et al. 1989; McCormick, unpublished observations). In this model the low-threshold  $\text{Ca}^{2+}$  spikes were similar in duration to those in rodent (Fig. 7, A and B) but substantially shorter in duration than those in cat (Fig. 7, C and D). The similarity of the modeled  $\text{Ca}^{2+}$  spikes to those in rodent is consistent with the fact that the model is based on voltage-clamp analysis of currents in rodent thalamocortical relay neurons (Huguenard and McCormick 1992).

Block of  $I_h$  in cat LGNd neurons with the local application of  $\text{Cs}^+$  results in a nearly complete abolition of the slow AHP occurring after the generation of a low-threshold  $\text{Ca}^{2+}$  spike (Fig. 7C; McCormick and Pape 1990a). Similarly, block of  $I_h$  in the model also resulted in a near abolition of the slow AHP (Fig. 7D), confirming that this electrophysiological feature of thalamocortical relay cells is generated largely by  $I_h$ . To summarize, the generation of a low-threshold  $\text{Ca}^{2+}$  spike is associated with a decrease in activation of  $I_h$  (as indicated by a decrease in  $m_h$ ; Fig. 7, B and D). On inactivation of  $I_T$  ( $h_T$  in Fig. 7, B and D), the membrane repolarizes and overshoots the original potential because of a decreased  $I_h$ . The subsequent increased activation of  $I_h$  ( $m_h$ , Fig. 7, B and D) results in a slow depolarization of the membrane potential back toward rest, thus generating an apparent AHP (Fig. 7, A and C).

#### Contribution of ionic currents to rhythmic $\text{Ca}^{2+}$ spike generation

Cat LGNd cells maintained in vitro, or hyperpolarized in vivo, generate rhythmic high-frequency burst discharges (Fig. 8A; McCormick and Pape 1990a; Steriade et al. 1991). We have previously proposed that these rhythmic burst discharges arise from the interaction of the low-threshold  $\text{Ca}^{2+}$  current  $I_T$  and the hyperpolarization-activated cation current  $I_h$  (McCormick and Pape 1990a). Here we examined the electrophysiological features of rhythmic burst firing with this model.

Intracellular recordings in rodent and cat LGNd cells in vitro reveal that cat LGNd cells have a much greater propensity toward slow rhythmic burst discharges than do rodent LGNd cells (McCormick, unpublished observations). This increased propensity may result in part from the substantially longer duration of cat low-threshold  $\text{Ca}^{2+}$  spikes in comparison to those of guinea pig or rat (e.g., Fig. 7). Indeed, we found here that the model thalamocortical relay cell would not support rhythmic burst firing unless the duration of the low-threshold  $\text{Ca}^{2+}$  spike was increased through either a reduction of the amplitude of  $I_{K2}$  (Fig. 4A) or a slowing of the kinetics of inactivation of  $I_T$  (not shown). Both of these methods of increasing the duration of the low-threshold spike resulted in the ability of the modeled cell to generate rhythmic  $\text{Ca}^{2+}$  spikes with similar characteristics. In this model, we chose to increase the duration of the low-threshold  $\text{Ca}^{2+}$  spike through reduction of  $I_{K2}$  (from 1 to  $0.2$   $\mu\text{S}$ ) because substantial differences in kinetics of cat and rodent T-currents have not yet been established.

Application of tetrodotoxin to cat LGNd cells maintained in vitro blocks voltage-dependent  $\text{Na}^+$  currents and reveals the underlying low-threshold  $\text{Ca}^{2+}$  spikes that sup-

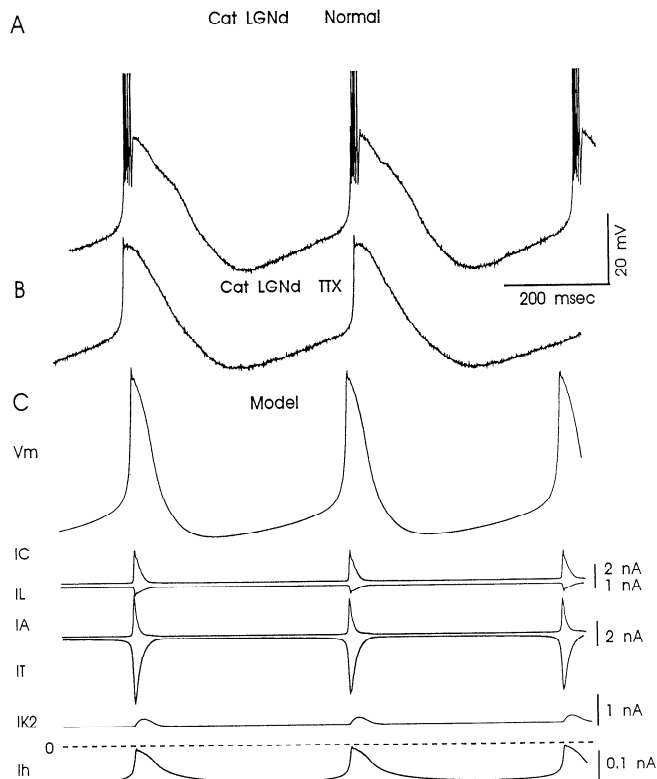


FIG. 8. Rhythmic burst firing in cat LGNd relay neurons and model of such. A and B: intracellular recording showing rhythmic oscillation of a cat LGNd cell in the lack of current injection before (A) and after (B) application of TTX ( $10$   $\mu\text{M}$  in micropipette). Note prominent "pacemaker" potential in between low threshold  $\text{Ca}^{2+}$  spikes. C: model of rhythmic oscillation in cat LGNd cells. Plot of the amplitude-time course of different currents reveals that  $\text{Ca}^{2+}$  spikes are generated by  $I_T$ ; their amplitude-time course is modulated by activation of  $I_C$ ,  $I_A$ , and  $I_{K2}$ ; and  $I_h$  generates the "pacemaker" potential in between low threshold  $\text{Ca}^{2+}$  spikes. Although  $I_h$  is a small current, it forms a dominant component of active currents in between  $\text{Ca}^{2+}$  spikes.

port rhythmic burst firing (Fig. 8, *A* and *B*; McCormick and Pape 1990a). These rhythmic  $\text{Ca}^{2+}$  spikes are characterized by the appearance of a “pacemaker” potential that slowly depolarizes the membrane potential in between  $\text{Ca}^{2+}$  spikes (Fig. 8*B*). Interestingly, the model of thalamo-cortical relay cells was able to support rhythmic burst firing and the generation of rhythmic low-threshold  $\text{Ca}^{2+}$  spikes at a frequency similar to that found in cat LGNd cells (0.5–4 Hz) (Fig. 8*C*). A plot of the different ionic currents flowing during the generation of rhythmic  $\text{Ca}^{2+}$  spikes revealed that each  $\text{Ca}^{2+}$  spike is generated largely by  $I_T$ , with a smaller contribution of  $I_L$ . As stated above, the  $\text{K}^+$  currents  $I_A$ ,  $I_C$ , and  $I_{K2}$  are all involved in the shaping of the amplitude-time course and repolarization of each  $\text{Ca}^{2+}$  spike. The hyperpolarization-activated cation current  $I_h$  forms only a small ionic current, with a peak amplitude in this example of  $\sim 100$  pA (Fig. 8*C*,  $I_h$ ). However, even though this ionic current is small, it exhibits substantial influence on the membrane potential in between each  $\text{Ca}^{2+}$  spike, owing to the near nonexistence of other voltage-dependent currents in between  $\text{Ca}^{2+}$  spikes (Fig. 8*C*). Thus  $I_h$  forms the “pacemaker” potential that slowly depolarizes the membrane potential in between  $\text{Ca}^{2+}$  spikes and activates each  $\text{Ca}^{2+}$  spike by activating  $I_T$ .

The contribution of each of the different ionic currents to rhythmic burst firing was examined by altering the maximal amplitude of the conductance underlying each current. Reduction of  $g_{\text{hmax}}$  to 0 nS resulted in an abolition of rhythmic oscillation and of the depolarizing “pacemaker” potential or “sag” on hyperpolarization (Fig. 9*A*). Increasing  $g_{\text{hmax}}$  to as little as 5 nS resulted in the appearance of rhythmic  $\text{Ca}^{2+}$  spikes (Fig. 9*A*). Increasing  $g_{\text{hmax}}$  to 10 nS increased the frequency of  $\text{Ca}^{2+}$  spike generation and decreased the amplitude of each  $\text{Ca}^{2+}$  spike (Fig. 9*B*). Further increases of  $g_{\text{hmax}}$  to 15 and 20 nS resulted in a failure to support rhythmic oscillation indefinitely, but rather resulted in damped oscillations that supported from four to seven cycles (Fig. 9, *C* and *D*).

Careful examination of the amplitude and time course of  $I_h$  and  $I_T$  and their underlying gates revealed the following sequence of events: at the starting membrane potential of  $-55$  mV very little  $g_h$  or  $g_T$  is active owing to the low level of  $m_h$  and the complete inactivation ( $h_T$ ) of  $g_T$  (Fig. 9*A*). As the membrane potential hyperpolarizes toward  $E_K$ ,  $I_h$  begins to activate (increase in  $m_h$ ) and the inactivation of  $I_T$  is largely removed (increase in  $h_T$ ) (Fig. 9*A*). Increases in  $m_h$  result in an increase in  $I_h$ , which subsequently depolarizes the membrane potential toward  $E_h$  ( $-40$  mV). The depolarization of the membrane eventually increases the activation of  $I_T$  ( $m_T$ ), which further depolarizes the membrane potential and further increases  $m_T$  in a positive feedback manner. Subsequently a low-threshold  $\text{Ca}^{2+}$  spike is generated. The increase in inactivation of  $I_T$  ( $h_T$ ) and the activation of  $I_A$ ,  $I_C$ , and  $I_{K2}$  results in the repolarization of the membrane and a subsequent increase in activation of  $I_h$  ( $m_h$ ; Fig. 9*A*). At low levels of  $g_{\text{hmax}}$  (5–10 nS), this oscillation quickly reached a steady state and continued indefinitely.

Increases in the amplitude of maximal  $g_h$  result in increases in the frequency of oscillation through an increase in the rate of rise of the membrane potential in between

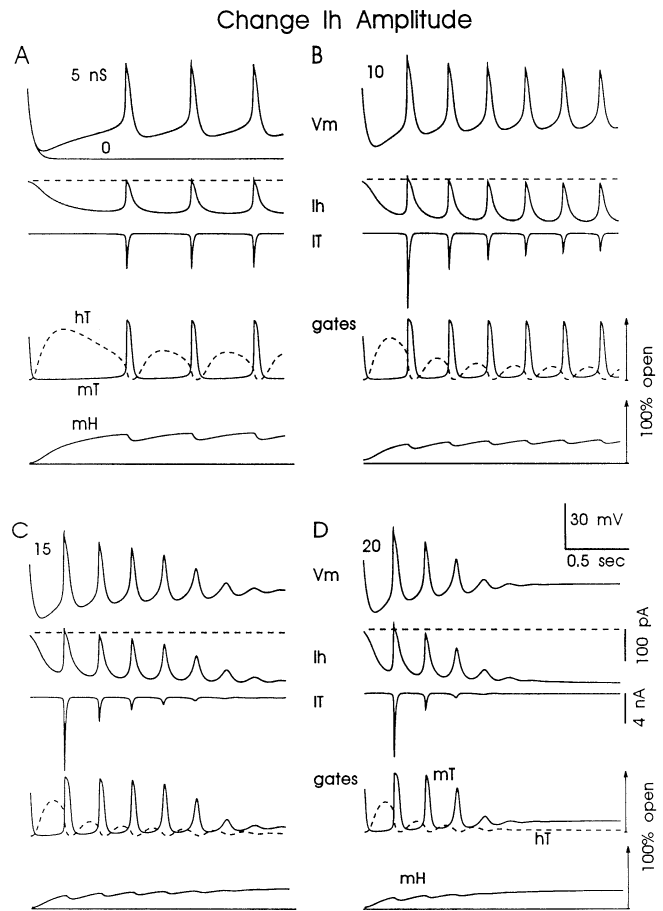


FIG. 9. Effect of changing  $I_h$  amplitude on rhythmic  $\text{Ca}^{2+}$  spike generation in the model cat LGNd relay cell. All simulations start at  $-55$  mV. If maximal h-conductance is 0 nS, then the cell fails to oscillate, but comes to rest at about  $-95$  mV. *A*: addition of 5 nS of  $g_{\text{hmax}}$  results in slow rhythmic  $\text{Ca}^{2+}$  spikes. Increase of  $g_{\text{hmax}}$  to 10 nS (*B*) increases the frequency of rhythmic  $\text{Ca}^{2+}$  spikes and decreases their amplitude. Increasing  $g_{\text{hmax}}$  to 15 or 20 nS results in a damped oscillation (*C* and *D*) because of the lack of sufficient removal of inactivation of  $I_T$  ( $h_T$ ,  $---$ ) and therefore a failure of the low threshold  $\text{Ca}^{2+}$  spikes.

subsequent  $\text{Ca}^{2+}$  spikes and consequently a decrease in the time interval before the next  $\text{Ca}^{2+}$  spike threshold is reached. However, increasing  $g_{\text{hmax}}$  past a critical level ( $\sim 12$  nS in this simulation) results in such a decrease in the depth of hyperpolarization of the membrane in between low-threshold  $\text{Ca}^{2+}$  spikes that the amount of inactivation of  $I_T$  that is removed is insufficient to maintain rhythmic oscillation (Fig. 9, *C* and *D*).

Increasing the amplitude of the maximal T-current permeability ( $p_T$ ) revealed that the model would support rhythmic  $\text{Ca}^{2+}$  spike generation only at values of  $\geq 40$  ( $\times 10^{-6}$  cm<sup>3</sup>/sec) or greater (Fig. 10). Increasing  $p_T$  from 40 to 80 was found to increase the frequency of rhythmic  $\text{Ca}^{2+}$  spike generation and increase the amplitude of each  $\text{Ca}^{2+}$  spike (Fig. 10, *B–D*). When  $p_T$  was set below 40, there was too little  $I_T$  available to support the continual generation of rhythmic  $\text{Ca}^{2+}$  spikes (Fig. 10*A*).

In addition to  $I_h$  and  $I_T$ , another important current in the generation of rhythmic  $\text{Ca}^{2+}$  spikes was  $I_{\text{Kleak}}$ . This current was important for drawing the membrane potential toward  $E_K$  in between  $\text{Ca}^{2+}$  spikes and therefore helping to remove

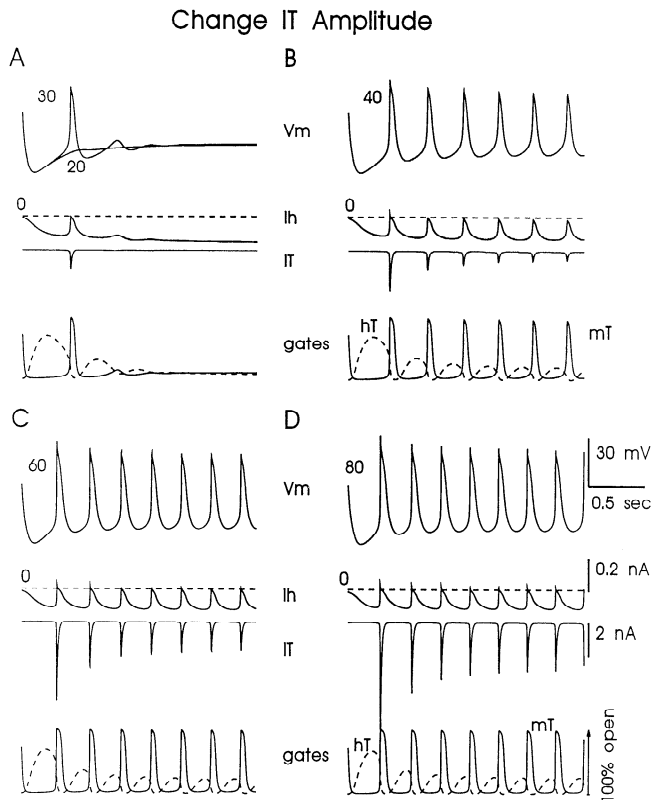


FIG. 10. Effect of changes in amplitude of  $I_T$  on rhythmic  $Ca^{2+}$  spike generation. With a  $p_T$  of 20 or 30 ( $\times 10^{-6}$  cm<sup>3</sup>/sec) the cell fails to oscillate. Increasing  $p_T$  from 40 to 80 increases the amplitude of the low threshold  $Ca^{2+}$  spikes and the frequency of oscillation.

inactivation of  $I_T$ . When  $g_{Kleak}$  was set to 4 nS, the modeled cell displayed only a damped oscillation owing to the lack of sufficient hyperpolarization in between sequential  $Ca^{2+}$  spikes (Fig. 11A). Increasing  $g_{Kleak}$  to 6 nS supported the generation of rhythmic  $Ca^{2+}$  spikes and slowed the frequency of their generation, whereas further increases to 8 nS further enhanced rhythmic  $Ca^{2+}$  spike generation and the amplitude of each  $Ca^{2+}$  spike. Additional increases of  $g_{Kleak}$  to 10 nS abolished the ability of the model to generate rhythmic  $Ca^{2+}$  spikes, owing to an inability of  $I_h$  to depolarize the membrane sufficiently to activate  $I_T$  (Fig. 11D).

These results reveal that the ability of thalamocortical relay neurons to generate rhythmic low-threshold  $Ca^{2+}$  spikes is a complex interaction requiring a balancing of the amplitude and properties of at least  $I_h$ ,  $I_T$ , and the conductances that determine the resting membrane potential and input resistance (e.g., leak conductances).

#### Effects of alteration in voltage dependence of $I_h$ on rhythmic $Ca^{2+}$ spike generation

Application of a variety of putative neurotransmitters to thalamocortical relay neurons in vitro results in alterations in the voltage dependency of  $I_h$  (McCormick and Pape 1990b; McCormick and Williamson 1991; Pape 1992). For example, activation of  $\beta$ -noradrenergic, serotonergic, or histaminergic- $H_2$  receptors results in a positive shift of the activation curve of  $I_h$  by 5–10 mV (McCormick and Pape

1990a; McCormick and Williamson 1991). In contrast, activation of adenosine- $A_1$  receptors appears to result in a shift in the activation curve of  $I_h$  to more negative membrane potentials (Pape 1992). Although preliminary evidence in vitro indicates that the positive shift in  $I_h$  activation results in the abolition of rhythmic burst firing (McCormick and Pape 1990b), this effect has not yet been studied in detail, particularly for small alterations in  $I_h$ . Therefore we examined here with the model of rhythmic  $Ca^{2+}$  spike generation the effect of alterations in the voltage dependency of  $I_h$ .

Shifts of the voltage dependence of  $I_h$  from  $-2.5$  to  $-10$  mV resulted in a slowing of the frequency of rhythmic  $Ca^{2+}$  spike generation and an increase in the amplitude of each  $Ca^{2+}$  spike (Fig. 12,  $-2.5$ ,  $-5.0$ ,  $-7.5$ , and  $-10.0$  mV). Likewise, shifting  $I_h$  voltage dependence by  $+2.5$  to  $+10$  mV resulted in an increase of the rate of rhythmic oscillation and a decrease in the amplitude of each  $Ca^{2+}$  spike (Fig. 12,  $2.5$ ,  $5.0$ ,  $7.5$ , and  $10.0$  mV). In addition, shifts of  $I_h$  by as little as 2.5 mV resulted in conversion of the rhythmic  $Ca^{2+}$  spike generation to a “damped oscillation” (Fig. 12,  $2.5$ ,  $5.0$ ,  $7.5$ , and  $10.0$  mV) as reported previously in cat LGNd thalamocortical neurons (McCormick and Pape 1990b). These results indicate that the neurotransmitter control of the voltage sensitivity of  $I_h$  may strongly influence the ability of thalamocortical relay neurons to gener-

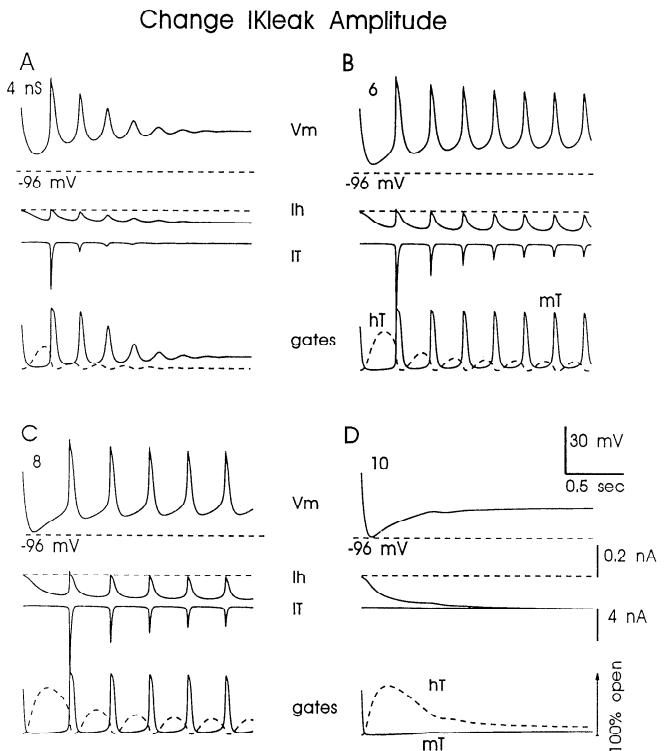


FIG. 11. Effect of changes in  $I_{Kleak}$  amplitude on the generation of low threshold  $Ca^{2+}$  spikes. *A*: with a  $g_{Kleak}$  of 4 nS, the model cell fails to maintain oscillation because of decreased hyperpolarization in between  $Ca^{2+}$  spikes and a subsequent decrease in the removal of inactivation of sufficient  $I_T$  to maintain oscillation. *B*: increasing  $g_{Kleak}$  to 6 nS results in maintained oscillation. *C*: increases to 8 nS slow the frequency of oscillation. *D*: increases to 10 nS block oscillation because of inability of  $I_h$  to depolarize the membrane sufficiently to activate a low threshold  $Ca^{2+}$  spike.

ate slow rhythmic  $\text{Ca}^{2+}$  spikes and the frequency with which these  $\text{Ca}^{2+}$  spikes occur.

#### Effect of rhythmic oscillation on response to depolarizing inputs

Extracellular recordings of LGNd neurons during the shift from sleep to waking reveal not only that there is a disappearance of rhythmic burst firing and the appearance of single spike activity, but also that the response of these neurons to visual inputs is also greatly enhanced (Coenen and Vendrik 1972; Livingstone and Hubel 1981). One possible reason for these changes in the responsiveness of LGNd relay cells is that the burst and single spike firing modes differ in their responsiveness to depolarizations associated with barrages of excitatory postsynaptic potentials from the retina. To investigate this possibility in this model, we examined the response of the model cell to the injection of a depolarizing current pulse while the cell either was rhythmically bursting or after tonic depolarization to near fast  $\text{Na}^+$  spike firing threshold.

Intracellular injection of a depolarizing current pulse during rhythmic burst firing resulted in a initial burst of action potentials resulting from the activation of  $I_T$  (Fig. 13B,  $\curvearrowright$ ) followed by a disruption of rhythmic oscillation because of tonic depolarization (Fig. 13B). The amplitude of the initial burst response depended on the amount of time which had passed since the  $\text{Ca}^{2+}$  spike before the injection

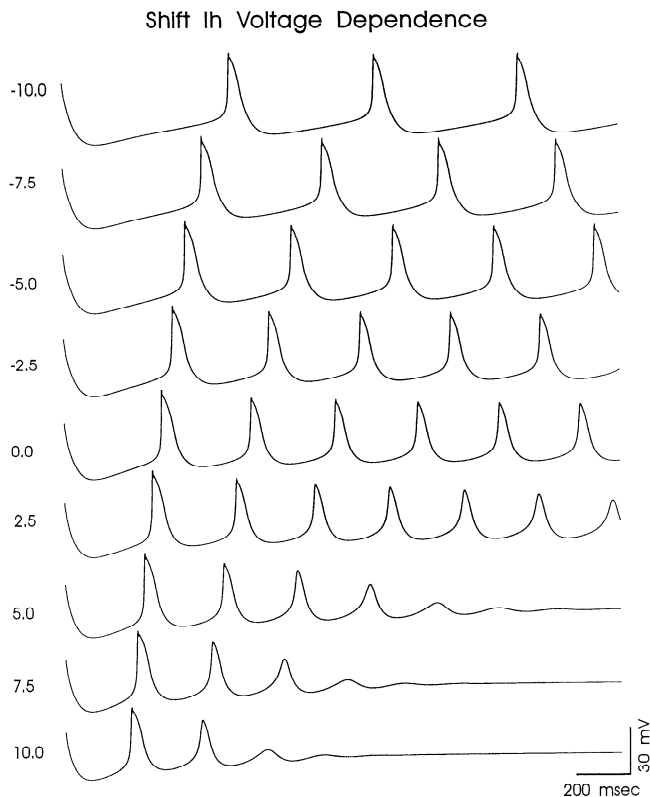


FIG. 12. Effect of changing  $I_h$  voltage dependence on rhythmic  $\text{Ca}^{2+}$  spike generation in model cat LGNd cell. Shifting  $I_h$  voltage dependence from 10 mV more negative ( $-10.0$ ) to 10 mV more positive ( $10.0$ ) results in substantial changes in the frequency of oscillation, amplitude of each  $\text{Ca}^{2+}$  spike, and the ability of the cell to maintain oscillation.

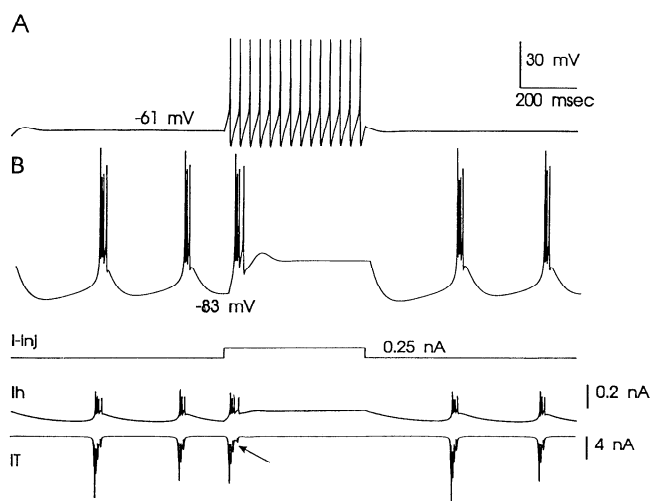


FIG. 13. Response of the model cell to a depolarizing current pulse ( $0.25$  nA) during oscillation and after reduction of  $I_{K\text{leak}}$ . *A*: reduction of  $g_{K\text{leak}}$  to  $2$  nS results in a new membrane potential of  $-61$  mV. Injection of a current pulse at this membrane potential results in a train of action potentials. *B*: increasing  $g_{K\text{leak}}$  to  $7$  nS results in the appearance of rhythmic burst firing. Injection of the same current pulse now results in only a transient burst at the beginning of the pulse because of activation of the low threshold  $\text{Ca}^{2+}$  current,  $I_T$  ( $\curvearrowright$ ). Current pulse also blocks the rhythmic oscillation.

tion of the current pulse (not shown). Decrease of  $g_{K\text{leak}}$  from  $7$  to  $2$  nS, as occurs in vitro in response to acetylcholine, norepinephrine, or histamine (McCormick 1992a; McCormick and Prince 1987; McCormick and Williamson 1991), resulted in a depolarization of the model cell to near firing threshold. Injection of the same depolarizing current pulse now resulted in a train of action potentials that showed little, if any, spike frequency adaptation (Fig. 13A).

Examination of the different ionic currents during the shift in firing mode from rhythmic bursting to single spike activity on reduction of  $I_{K\text{leak}}$  revealed that the persistent  $\text{Na}^+$  current  $I_{\text{Nap}}$  was particularly important in facilitating the depolarization of the membrane sufficiently to bring the membrane to, or close to, single spike firing threshold.

#### DISCUSSION

Intracellular recordings in vivo and in vitro from thalamocortical relay neurons have shown that these cells possess a number of unique electrophysiological properties, including the ability to generate high frequency burst discharges on removal of hyperpolarization (Deschênes et al. 1984; Jahnsen and Llinás 1984a,b); tonic firing during depolarization that displays little, if any, spike frequency adaptation (Jahnsen and Llinás 1984a; McCormick 1992a); apparent rectification at rest, in which the response to depolarizing current pulses is considerably smaller than that to hyperpolarizing current pulses (McCormick 1991); and finally, the ability to generate intrinsic rhythmic burst firing at interburst frequencies of  $0.5$ – $4$  Hz (Curró Dossi et al. 1991; Leresche et al. 1991; McCormick and Pape 1990a; Soltesz et al. 1991; Steriade et al. 1992). These electrophysiological features of thalamocortical relay neurons have been proposed to underlie the different modes of action potential generation that thalamocortical relay neurons dis-

play *in vivo*, particularly in the transition from rhythmic burst firing to tonic activity associated with the transition from slow wave sleep to waking or to rapid-eye-movement sleep (reviewed in Steriade and Deschênes 1984; Steriade and Llinás 1988). The present model of thalamocortical relay neurons successfully replicated all of the above-listed electrophysiological features of these cells.

#### *Rebound burst discharges*

As revealed by *in vitro* experiments in thalamocortical relay neurons (Coulter et al. 1989; Crunelli et al. 1989; Jahnsen and Llinás 1984a,b; Hernández-Cruz and Pape 1989), our results confirm the central role of the low-threshold  $\text{Ca}^{2+}$  spike in the generation of rebound high frequency burst discharges on the release of a phasic hyperpolarization. In addition, the present simulation of low-threshold  $\text{Ca}^{2+}$  spikes suggests that this electrophysiological response is considerably influenced by the amplitude and time course of various voltage- and  $\text{Ca}^{2+}$ -dependent  $\text{K}^+$  currents. In particular, the transient and rapidly inactivating  $\text{K}^+$  current  $I_A$  (Huguenard et al. 1991) appears to be particularly involved in the rising phase of the low-threshold  $\text{Ca}^{2+}$  spike, whereas the more slowly inactivating  $\text{K}^+$  current  $I_{K2}$  (Huguenard and Prince 1991) controls the repolarizing phase of the  $\text{Ca}^{2+}$  spike (Fig. 4A). The possibility that transient  $\text{K}^+$  currents may control the shape of the low-threshold  $\text{Ca}^{2+}$  spike has recently received experimental support with *in vitro* experiments in which the bath application of 100  $\mu\text{M}$  4-AP, which abolishes the slowly inactivating  $\text{K}^+$  current  $I_{AS}$ , resulted in an increase in the duration of the low-threshold  $\text{Ca}^{2+}$  spike and an increase in its peak amplitude (see Fig. 4D; McCormick 1991). In addition, in the present model, the  $\text{Ca}^{2+}$ -activated  $\text{K}^+$  current also contributed substantially to the shaping of the low-threshold  $\text{Ca}^{2+}$  spike, particularly during the most depolarized membrane potentials, owing to the voltage dependency of this current and the activation of the high threshold  $\text{Ca}^{2+}$  current.

An interesting, and potentially important, finding of this simulation and those of others (Yamada et al. 1989) concerns the interpretation of current-clamp recordings when an ionic current is reduced or blocked. In the present model, a decrease in any one or two of the voltage-dependent  $\text{K}^+$  currents resulted in an increase in the remaining  $\text{K}^+$  currents in response to a depolarizing event (e.g., fast action potential,  $\text{Ca}^{2+}$  spike, or current injection), owing to the increased depolarization of the cell. This compensatory increase in the remaining  $\text{K}^+$  currents could result in a substantially smaller change in the membrane potential than expected based merely on the amplitude of the blocked current alone (e.g., Fig. 4, A and B). Results obtained with current-clamp recordings *in vitro* must, therefore, take into account this potential difficulty of interpretation.

#### *Tonic firing*

Modeling of the response of thalamocortical relay neurons to tonic depolarization revealed trains of fast action potentials that display relatively little spike frequency adaptation (e.g., Figs. 2 and 5). Examination of the different

ionic currents involved in fast action potential generation revealed that each spike was generated by the fast  $\text{Na}^+$  current  $I_{\text{Na}}$  with an additional contribution by the high-threshold  $\text{Ca}^{2+}$  current  $I_L$ . The subsequent activation of  $I_C$  (with an additional contribution by  $I_A$  and  $I_{K2}$ ) resulted in repolarization of each action potential. The exact contribution of each of these different  $\text{K}^+$  currents in the repolarization of action potentials in thalamic relay neurons remains to be examined, particularly because the  $\text{Ca}^{2+}$ -activated  $\text{K}^+$  conductances of these cells have not yet been characterized. It may be that the relative contributions of  $I_A$ ,  $I_{K2}$ , and  $\text{Ca}^{2+}$ -activated  $\text{K}^+$  currents to repolarization of fast action potentials in thalamic relay cells are substantially different from those modeled here. In other neuronal cell types, most notably hippocampal pyramidal cells and sympathetic ganglion cells, the repolarization of fast action potentials is achieved through the activation of a variety of  $\text{K}^+$  currents, of which  $\text{Ca}^{2+}$ -activated  $\text{K}^+$  currents appear to contribute a major role at depolarized membrane potentials (e.g., positive to  $-60$  mV; Belluzzi and Sacchi 1988, 1991; Lancaster and Nicoll 1987; Storm 1987). The lack of spike frequency adaptation in LGNd neurons and this model presumably results from the apparent lack of the slow  $\text{Ca}^{2+}$ -activated  $\text{K}^+$  current known as  $I_{\text{AHP}}$  in these cells (see Madison and Nicoll 1984; Pennefather et al. 1985). Indeed, relay neurons of the parateanial thalamic nucleus display both a substantial slow afterhyperpolarizing current and spike frequency adaptation (McCormick and Prince 1988; McCormick, unpublished observations). The lack of significant spike frequency adaptation in LGNd relay cells presumably allows these cells to relay trains of action potentials from the retina to the visual cortex for prolonged periods of time without decay.

#### *Apparent rectification*

Previous *in vitro* intracellular recordings from thalamocortical relay neurons have suggested that the activation of various  $\text{K}^+$  currents may be involved in decreasing the response of these cells to phasic or tonic depolarization (McCormick 1991). Our results confirm and extend this hypothesis and reveal that depolarization from resting membrane potentials typical for those obtained with intracellular recordings *in vitro* or *in vivo* may result in the activation of  $I_A$ ,  $I_{K2}$ , and  $I_C$ , all of which subsequently can reduce the amplitude of the electrotonic response. In particular, the activation of the more slowly inactivating or non-inactivating currents  $I_{K2}$  and  $I_C$  is important to the reduction of the response to prolonged ( $>50$  ms) depolarization.

The ability of thalamocortical relay cells to display reduced responsiveness to depolarization and the apparent favoring of response to hyperpolarization may explain in part the observation that thalamocortical relay neurons are highly responsive to inhibitory postsynaptic potentials during periods of slow wave sleep, while being considerably less responsive to excitatory postsynaptic potentials (reviewed in Steriade and Deschênes 1984; Steriade and Llinás 1988). In contrast, tonic depolarization of thalamocortical relay neurons, such as that which occurs during the waking state (Hirsch et al. 1983), abolishes this bias such that the neu-

ron responds to depolarizing and hyperpolarizing current pulses in a more equitable manner (McCormick 1991). This intrinsic bias at hyperpolarized membrane potentials in favor of rebound burst discharges to inhibitory postsynaptic potentials and the lack of firing to excitatory postsynaptic potentials may facilitate the appearance of intrathalamic rhythmic burst firing and the filtering, or lack of responsiveness, to excitatory postsynaptic potentials of retinal or cortical origin during periods of slow wave sleep. In addition, the electroresponsive properties of thalamic neurons during endogenous rhythmic burst firing results in an emphasis of the initial portions of depolarizations with a lack of response to prolonged events (i.e., Fig. 13). It remains to be determined whether this emphasis of low-frequency transient events is of value in the processing of sensory information (see discussion in McCormick and Feuser 1990).

#### *Intrinsic rhythmic burst firing*

The ability of cat thalamocortical relay neurons to generate intrinsic rhythmic burst firing in the frequency range of 0.5–4 Hz has been suggested to result from the interplay of the low-threshold  $\text{Ca}^{2+}$  current  $I_T$  and the hyperpolarization-activated cation current  $I_h$  (McCormick and Pape 1990a; Soltesz et al. 1991). The model of thalamocortical relay neurons confirmed that it is possible to support rhythmic  $\text{Ca}^{2+}$  spike generation based solely on the presence of these two currents, with the addition of leak currents to determine the membrane potential and apparent input resistance. Examination of the actions of the different ionic currents in the present model revealed that rhythmic  $\text{Ca}^{2+}$  spike generation undergoes a regular and repeating sequence of events in which the  $\text{Ca}^{2+}$  spike is activated by  $I_T$  and the “pacemaker” potential is generated by  $I_h$  (Figs. 8–11). One of the most important factors involved in the generation of rhythmic  $\text{Ca}^{2+}$  spike generation was the amount of T-current permeability ( $p_T$ ) available before activation of each  $\text{Ca}^{2+}$  spike. If the amount of  $p_T$  available (i.e., not inactivated) became too small, then rhythmic  $\text{Ca}^{2+}$  spike generation eventually failed and the neuron displayed a “damped” oscillation. The amount of  $p_T$  available before each  $\text{Ca}^{2+}$  spike generated depends on two important factors: the maximal T-current permeability present in the neuron and the depth and duration of the hyperpolarization, and therefore the degree of removal of inactivation of  $I_T$ , before the  $\text{Ca}^{2+}$  spike. The depth and duration of the hyperpolarization before the  $\text{Ca}^{2+}$  spike depended in this model on the amplitude and kinetics of  $I_h$  and the amplitude of the leak currents  $I_{\text{Kleak}}$  and  $I_{\text{Naleak}}$ . Increasing the amplitude of  $I_h$  or shifting its voltage dependence to more positive membrane potentials leads to a decrease in the duration and depth of hyperpolarization in between rhythmic  $\text{Ca}^{2+}$  spikes and therefore to an increase in the frequency of oscillation and a decrease in the amplitude of each  $\text{Ca}^{2+}$  spike. Similar results have been obtained from cat LGNd neurons in vitro. Local extracellular application of  $\text{Cs}^+$ , which reduces  $I_h$ , results in hyperpolarization of these cells, a dramatic increase in the amplitude of the low-threshold  $\text{Ca}^{2+}$  spike (and therefore an increase in the number of  $\text{Na}^+$

spikes generated), and a slowing of the frequency of oscillation (McCormick and Pape 1990a).

Activation of  $\beta$ -adrenergic receptors,  $\text{H}_2$ -histaminergic receptors, and serotonergic receptors all result in positive shifts in the voltage dependence of  $I_h$  and in the activation kinetics of this current (McCormick and Pape 1990b; McCormick and Williamson 1991). Similarly, activation of adenylate cyclase or increases in intracellular concentrations of cyclic adenosine monophosphate (cAMP) have similar effects, suggesting that the above-mentioned receptors may alter  $I_h$  through this second messenger. Although we have previously proposed that maximal (5–10 mV) shifts in the voltage dependence of  $I_h$  abolish the ability of thalamocortical relay cells to rhythmically burst (McCormick and Pape 1990b), the effect of more subtle alterations in  $I_h$  has not yet been examined. In this model, we found that subtle (mV) alteration in the voltage dependence of  $I_h$  can strongly influence the rate of rhythmic  $\text{Ca}^{2+}$  spike generation from a frequency of 0.5 to one of  $\sim 4$  Hz (Fig. 12). Thus the activity of brainstem monoaminergic neurons and hypothalamic histaminergic cells may control in part the frequency and propensity with which thalamocortical cells generate rhythmic burst firing through alterations in the voltage dependence of  $I_h$ .

#### *Comparison with other thalamic models*

Over the past few years a number of other mathematical models of thalamic neurons have been published that successfully mimicked one or more features of thalamic relay cells, including the generation of low-threshold  $\text{Ca}^{2+}$  spikes (Dextexhe and Babloyantz 1991; Rose and Hindmarsh 1985, 1989; Wang et al. 1991) and the generation of tonic single spike firing on depolarization (Rose and Hindmarsh 1989; McMullen and Ly 1988). However, these models were limited owing to the limited information available on the different ionic currents present in thalamocortical relay cells. In addition, the ability of thalamic relay cells to oscillate intrinsically has been demonstrated only recently, along with the appreciation of the importance of the hyperpolarization-activated cation current in this oscillation (e.g., McCormick and Pape 1990a). Like previous models, these simulations successfully replicated the presence of two firing modes in thalamic relay neurons: burst firing and single spike activity. However, in addition, this model also predicted the presence of slow-frequency rhythmic behavior, apparent rectification of the membrane potential at rest, and the contribution of the various  $\text{K}^+$  currents to the amplitude-time course of the low-threshold  $\text{Ca}^{2+}$  spikes.

The similarity between rhythmic low-threshold  $\text{Ca}^{2+}$  spike generation in this model of thalamocortical relay cells and the proposed mechanisms of rhythm generation in cardiac cells is striking and deserves comment. DiFrancesco and Noble (1985, 1989) have presented a model of cardiac pacemaking in which the hyperpolarization-activated cation current  $I_f$  makes an important contribution to the “pacemaker” potential. This current contributes to the determination of the frequency of rhythmic activity in that it activates on hyperpolarization in between action potentials and repolarizes the membrane toward threshold for genera-

tion of the next action potential. A number of neuromodulatory substances alter the voltage sensitivity of  $I_f$ , much in the same manner as  $I_h$  (see DiFrancesco 1985; DiFrancesco et al. 1989; DiFrancesco and Tortora 1991). For example, activation of cyclic AMP or stimulation of  $\beta$ -adrenergic receptors results in a marked enhancement of  $I_f$  through a positive shift in its voltage sensitivity (DiFrancesco and Tortora 1991), as it does  $I_h$  in thalamic relay cells (McCormick and Pape 1990a). These similarities suggest that hyperpolarization-activated cation currents may have a general role in the generation of rhythmic oscillation in various types of electrically excitable cells.

#### APPENDIX

The model of thalamocortical relay cell was constructed using the following equations. The principal equation describing the change in intracellular potential with respect to time was

$$dV/dt = -(I_{inj} + I_{Na} + I_{Nap} + I_L + I_T + I_C + I_A + I_{K2} + I_h + I_{Kleak} + I_{Naleak})/C_{in} \quad (A1)$$

The input capacitance ( $C_{in}$ ) was set to 0.29 nF, as was measured in a cat LGNd neuron that generated rhythmic burst firing and that is illustrated in Fig. 8. In all equations voltage is in millivolts, current is in nanoamperes, time is in milliseconds, conductance is microsiemens (unless stated otherwise), concentration is molar, and volume is in liters.

The mathematical description of the different currents was achieved either through a Hodgkin-Huxley style derivation of forward and backward rate equations (Hodgkin and Huxley 1952) or through the mathematical description of the voltage dependence of activation and inactivation and the kinetics of such. The equations for  $I_A$ ,  $I_{K2}$ ,  $I_T$ , and  $I_h$  were derived from voltage-clamp recordings of thalamocortical relay neurons and are given in the accompanying paper (Huguenard and McCormick 1992). The range in maximal conductances for these four currents as observed in vitro and the values used in the present model are presented in Table 1. Here we present the equations for the description of  $I_{Na}$ ,  $I_{Nap}$ ,  $I_L$ ,  $I_C$ ,  $I_{Kleak}$ , and  $I_{Naleak}$  and for  $Ca^{2+}$  buffering, assuming a temperature of 23.5°C.

#### $I_{Na}$

The transient  $Na^+$  current,  $I_{Na}$ , was described by the following Hodgkin-and-Huxley-style equations

$$I_{Na} = g_{Namax} \cdot (E - E_{Na}) \cdot m^3 h \quad (A2)$$

where  $g_{Namax}$  is the maximal conductance,  $E$  is the membrane potential,  $E_{Na}$  is the equilibrium potential for  $Na^+$  (assumed to be +45 mV),  $m$  is the activation variable and varies from 0 (not activated) to 1 (fully activated), and  $h$  is the inactivation variable and also varies from 0 (completely inactivated) to 1 (no inactivation). In all Hodgkin-and-Huxley-style descriptions, the steady-state activation or inactivation variables were described by

$$m_\infty(h_\infty) = \alpha / (\alpha + \beta) \quad (A3)$$

and the time constant,  $\tau$ , of activation or inactivation was described by

$$\tau = 1 / (\alpha + \beta) \quad (A4)$$

For the activation variable  $m$  of  $I_{Na}$ ,  $\alpha$  and  $\beta$  were as follows

$$\alpha = 0.091 \cdot (V_m + 38) / \{1 - \exp[-(V_m + 38)/5]\} \quad (A5)$$

$$\beta = -0.062 \cdot (V_m + 38) / \{1 - \exp[(V_m + 38)/5]\} \quad (A6)$$

The inactivation variable  $h$  was described by

$$\alpha = 0.016 \cdot \exp[(-55 - V_m)/15] \quad (A7)$$

$$\beta = 2.07 / \{\exp[(17 - V_m)/21] + 1\} \quad (A8)$$

These parameters were derived from the data of Huguenard et al. (1988) obtained from cortical pyramidal cells. The maximal conductance,  $g_{Namax}$ , for this current was set to 12  $\mu S$  in accordance with the model of  $Na^+$  action potentials by Beluzzi and Sacchi (1991).

#### $I_{Nap}$

$I_{Nap}$  was described by

$$I_{Nap} = g_{Napmax} \cdot (E - E_{Na}) \cdot m \quad (A9)$$

The voltage dependence of activation of the persistent  $Na^+$  current was described by the Boltzman equation

$$m_{Nap,\infty} = 1 / \{1 + \exp[(-49 - V_m)/5]\} \quad (A10)$$

This equation is that derived by French et al. (1990) on the basis of data obtained from hippocampal pyramidal cells. The kinetics of activation of  $g_{Nap}$  are not yet available, although it is known to activate rapidly in cortical pyramidal neurons (Stafstrom et al. 1985). Here we assumed the same kinetics for activation for  $g_{Nap}$  as for  $g_{Na}$ . The maximal conductance for  $g_{Nap}$  was set to 7 nS, in accordance with the data of French et al. (1990).

#### $I_C$

The  $Ca^{2+}$ -activated  $K^+$  current  $I_C$  was described by the equation of Yamada et al. (1989) derived for bullfrog sympathetic ganglion cells

$$I_C = g_{Cmax} \cdot (E - E_K) \cdot m \quad (A11)$$

and

$$\alpha = 2.5 \times 10^5 \cdot [Ca^{2+}]_i \cdot \exp(V_m/24) \quad (A12)$$

$$\beta = 0.1 \cdot \exp(-V_m/24) \quad (A13)$$

where  $E_K$  was assumed to be -105 mV, according to the data of McCormick and Prince (1987). The maximal conductance for  $I_C$  was set to 1  $\mu S$ , which is within the range proposed in other models of  $Na^+$ -dependent action potentials (Belluzzi and Sacchi 1991; Yamada et al. 1989). Intracellular recordings in vitro from thalamocortical relay neurons reveal that fast action potentials and high threshold  $Ca^{2+}$  spikes are followed by substantial  $Ca^{2+}$ -activated  $K^+$  currents, whereas low-threshold  $Ca^{2+}$  spikes are not (Jahnsen and Llinás 1984a,b; McCormick, unpublished observations). In accordance with this data, we made  $I_C$  sensitive to increases in  $Ca^{2+}$  concentration resulting from  $I_L$ , but not those resulting from  $I_T$ . Recent immunological studies have revealed the spatial segregation of L-type channels in hippocampal pyramidal cells (Westenbroek et al. 1990), confirming at least the possibility that L- and T-type  $Ca^{2+}$  channels are segregated from one and another in thalamic neurons and therefore may differentially activate  $Ca^{2+}$ -activated  $K^+$  currents.

#### $I_L$

As with the low-threshold  $Ca^{2+}$  current (Eq. 10 in Huguenard and McCormick 1992), the high-threshold  $Ca^{2+}$  was modeled using the Goldman-Hodgkin-Katz constant field equation

$$I_L = p_{Lmax} \cdot m^2 \cdot z^2 \cdot EF^2/RT \cdot ([Ca^{2+}]_i - [Ca^{2+}]_o \cdot \exp(-zFE/RT)) / [1 - \exp(-zFE/RT)] \quad (A14)$$

where  $p_{Lmax}$  is the maximal permeability (in  $\text{cm}^3/\text{sec}$ ),  $z$  is 2 for  $\text{Ca}^{2+}$ ,  $[Ca^{2+}]_i$  is determined by both  $I_L$  and  $I_T$ ,  $[Ca^{2+}]_o$  is 2.0 mM, and  $E$ ,  $F$ ,  $R$ , and  $T$  have their usual meanings (Hille 1984).

The activation variable  $m$  was described according to the data of Kay and Wong (1987) obtained from hippocampal pyramidal cells

$$\alpha = 1.6 / \{1 + \exp[-0.072 \cdot (V - 5.0)]\} \quad (A15)$$

$$\beta = 0.02 \cdot (V - 1.31) / \{\exp[(V - 1.31)/5.36] - 1\} \quad (A16)$$

In dissociated thalamocortical relay cells,  $p_L$  was generally twice as large as  $p_T$ . Therefore, because  $p_T$  was set at  $40 (\times 10^{-6} \text{ cm}^3/\text{sec})$ ,  $p_L$  was set to  $80 (\times 10^{-6} \text{ cm}^3/\text{sec})$ .

### $\text{Ca}^{2+}$ buffering

Calcium concentrations were calculated in the inner 100 nm of cytoplasm just beneath the membrane area of  $29,000 \mu\text{m}^2$ . In this simulation, we adopted the simple proportional model of  $\text{Ca}^{2+}$  diffusion out of this space used by Traub (1982) in the modeling of hippocampal pyramidal cells. In this model, the change in  $[Ca^{2+}]_i$  is described by

$$d[Ca^{2+}]/dt = \beta \cdot [Ca^{2+}] \quad (A17)$$

The concentration of  $\text{Ca}^{2+}$  at time step  $t$  was then calculated according to

$$[Ca^{2+}]_t = [Ca^{2+}]_{t-1} + \Delta t \cdot \{[-5.18 \times 10^{-3} \cdot (I_T \text{ or } I_L)] / (\text{area} \cdot \text{depth}) - \beta \cdot [Ca^{2+}]_{t-1}\} \quad (A18)$$

where the constant  $-5.18 \times 10^{-3}$  is used to convert current (in nanoamperes), time (in milliseconds), and volume (in cubic micrometers) to concentration of  $\text{Ca}^{2+}$  ions and is derived from

$$1 \text{ nA} = 1 \times 10^{-12} \text{ Coulombs/msec}$$

$$1 \text{ liter} = 1 \times 10^{15} \mu\text{m}^3$$

and Faraday's constant of  $1.92988 \times 10^5$  coulombs per mole  $\text{Ca}^{2+}$ .

The minimal  $[Ca^{2+}]_i$  was set to 50 nM. The low-threshold and high-threshold  $\text{Ca}^{2+}$  currents were treated separately.

The diffusion rate constant  $\beta$  was adjusted so as to replicate the duration of the AHP after a single action potential ( $\sim 60$  ms). A value for  $\beta$  of 1 was used in these simulations at  $355^\circ\text{C}$ .

### $I_{Kleak}$ and $I_{Naleak}$

The leak conductances  $g_{Kleak}$  and  $g_{Naleak}$  were considered to be linear leak conductances and were described by

$$I_{Kleak} = g_{Kleak} \cdot (E - E_K) \quad (A19)$$

$$I_{Naleak} = g_{Naleak} \cdot (E - E_{Na}) \quad (A20)$$

The maximal conductances  $g_{Kleak}$  and  $g_{Naleak}$  were adjusted to match the resting membrane potential and apparent input conductance of guinea pig or cat LGNd that was being modeled. In the modeling of guinea pig neurons, this resulted in a  $g_{Kleak}$  of 15 nS and a  $g_{Naleak}$  of 6 nS (see RESULTS). In the modeling of the oscillating cat LGNd neuron, two properties of this cell were considered: 1) after the block of  $I_h$  with the local application of  $\text{Cs}^+$ , the resting membrane potential of this cell was approximately  $-85$  mV and the apparent input resistance was 150 M $\Omega$ . In the present model,  $g_{Kleak}$  was set to 7 nS and  $g_{Naleak}$  was set to 0.25 nS, giving a

resting membrane potential of  $-95$  mV and an apparent input resistance of 138 M $\Omega$ .

We thank B. Strowbridge, P. Majherate, and G. Shepherd, whose advice made the present model of thalamic neurons possible.

This work was supported by National Institute of Neurological Disorders and Stroke Grants NS-06477 and NS-12151 to D. A. Prince and NS-26143 to D. A. McCormick. Additional support was obtained from the Sloan Foundation, the Klingenstein Fund, and the Jane and Peter Pattison Fund.

Those interested in obtaining a copy of the modelling program and instruction manual should send a diskette and an address label to J. R. Huguenard or D. A. McCormick.

Address for reprint requests: D. A. McCormick, Section of Neurobiology, SHM C303, Yale Medical School, 333 Cedar St., New Haven, CT 06510.

Received 24 March 1992; accepted in final form 8 June 1992.

### REFERENCES

- BELLUZZI, O. AND SACCHI, O. The interactions between potassium and sodium currents in generating action potentials in the rat sympathetic neuron. *J. Physiol. Lond.* 397: 127-147, 1988.
- BELLUZZI, O. AND SACCHI, O. A five-conductance model of the action potential in rat sympathetic neuron. *Prog. Biophys. Mol. Biol.* 55: 1-30, 1991.
- BLOOMFIELD, S. A., HAMOS, J. E., AND SHERMAN, S. M. Passive cable properties and morphological correlates of neurons in the lateral geniculate nucleus of the cat. *J. Physiol. Lond.* 383: 653-692, 1987.
- COENEN, A. M. L. AND VENDRIK, A. J. H. Determination of the transfer ratio of cat's geniculate neurons through quasi-intracellular recordings and the relation with the level of alertness. *Exp. Brain Res.* 14: 227-242, 1972.
- COULTER, D. A., HUGUENARD, J. R., AND PRINCE, D. A. Calcium currents in rat thalamocortical relay neurons: kinetic properties of the transient, low-threshold current. *J. Physiol. Lond.* 414: 587-604, 1989.
- CRUNELLI, V., LIGHTOWLER, S., AND POLLARD, C. E. A T-type  $\text{Ca}^{2+}$  current underlies low-threshold  $\text{Ca}^{2+}$  potentials in cells of the cat and rat lateral geniculate nucleus. *J. Physiol. Lond.* 413: 543-561, 1989.
- CURRÓ DOSSI, R., NÚÑEZ, A., AND STERIADE, M. Electrophysiology of a slow intrinsic oscillation in thalamocortical cells of cat in vivo. *J. Physiol. Lond.* In press, 1991.
- DESCHÊNES, M., PARADIS, M., ROY, J. P., AND STERIADE, M. Electrophysiology of neurons of lateral thalamic nuclei in rat: resting properties and burst discharges. *J. Neurophysiol.* 51: 1196-1219, 1984.
- DETXEHE, A. AND BABLOYANTZ, A. Cortical coherent activity induced by thalamic oscillations. In: *Complex Dynamics in Neural Networks*, edited by J. Taylor. New York: Springer-Verlag, 1991.
- DI FRANCESCO, D. The cardiac hyperpolarizing-activated current  $I_f$ : origins and developments. *Prog. Biophys. Mol. Biol.* 46: 163-183, 1985.
- DI FRANCESCO, D. The contribution of the "pacemaker" current ( $i_f$ ) to generation of spontaneous activity in rabbit sino-atrial node myocytes. *J. Physiol. Lond.* 434: 23-40, 1991.
- DI FRANCESCO, D., DUCOURET, P., AND ROBINSON, R. B. Muscarinic modulation of cardiac rate at low acetylcholine concentrations. *Science Wash. DC* 243: 669-671, 1989.
- DI FRANCESCO, D. AND NOBLE, D. A model of cardiac electrical activity incorporating ionic pumps and concentration changes. *Philos. Trans. R. Soc. Lond. B Biol. Sci.* 307: 353-398, 1985.
- DI FRANCESCO, D. AND NOBLE, D. Current  $I_f$  and its contribution to cardiac pacemaking. In: *Neuronal and Cellular Oscillators*, edited by J. W. Jacklet. New York: Dekker, 1989, p. 31-57.
- DI FRANCESCO, D. AND TORTORA, P. Direct activation of cardiac pacemaker channels by intracellular cyclic AMP. *Nature Lond.* 351: 145-147, 1991.
- FRENCH, C. R., SAH, P., BUCKETT, K. J., AND GAGE, P. W. A voltage-dependent persistent sodium current in mammalian hippocampal neurons. *J. Gen. Physiol.* 95: 1139-1157, 1990.
- HAMILL, O. P., HUGUENARD, J. R., AND PRINCE, D. A. Patch-clamp studies of voltage-gated currents in identified neurons of the rat cerebral cortex. *Cerebral Cortex* 1: 48-61, 1991.

- HERNÁNDEZ-CRUZ, A. AND PAPE, H.-C. Identification of two calcium currents in acutely dissociated neurons from the rat lateral geniculate nucleus. *J. Neurophys.* 61: 1270–1283, 1989.
- HILLE, B. Ionic channels of excitable membranes. Sunderland, MA: Sinauer, 1984.
- HIRSCH, J. C., FOURMENT, A., AND MARC, M. E. Sleep-related variations of membrane potential in the lateral geniculate body relay neurons of the cat. *Brain Res.* 259: 308–312, 1983.
- HODGKIN, A. L. AND HUXLEY, A. F. A quantitative description of membrane current and its application to conduction and excitation in nerve. *J. Physiol. Lond.* 117: 500–544, 1952.
- HUGUENARD, J. R., COULTER, D. A., AND PRINCE, D. A. A fast transient potassium current in thalamic relay neurons: kinetics of activation and inactivation. *J. Neurophysiol.* 66: 1304–1315, 1991.
- HUGUENARD, J. R., HAMILL, O. P., AND PRINCE, D. A. Developmental changes in Na<sup>+</sup> conductances in rat neocortical neurons: appearance of a slowly inactivating component. *J. Neurophysiol.* 59: 778–795, 1988.
- HUGUENARD, J. R. AND MCCORMICK, D. A. Simulation of the currents involved in rhythmic oscillations in thalamic relay neurons. *J. Neurophysiol.* 68: 1373–1383, 1992.
- HUGUENARD, J. R. AND PRINCE, D. A. Slow inactivation of a TEA-sensitive K current in acutely isolated rat thalamic relay neurons. *J. Neurophysiol.* 66: 1316–1328, 1991.
- JAHNSEN, H. AND LLINÁS, R. Electrophysiological properties of guinea-pig thalamic neurons: an in vitro study. *J. Physiol. Lond.* 349: 205–226, 1984a.
- JAHNSEN, H. AND LLINÁS, R. Ionic basis for the electroresponsiveness and oscillatory properties of guinea-pig thalamic neurons in vitro. *J. Physiol. Lond.* 349: 227–247, 1984b.
- KAY, A. R. AND WONG, R. K. S. Calcium current activation kinetics in isolated pyramidal neurons of the CA1 region of the mature guinea-pig hippocampus. *J. Physiol. Lond.* 392: 603–616, 1987.
- LANCASTER, B. AND NICOLL, R. A. Properties of two calcium-activated hyperpolarizations in rat hippocampal neurons. *J. Physiol. Lond.* 389: 187–203, 1987.
- LERESCHE, N., LIGHTOWLER, S., SOLTESZ, I., JASSIK-GERSCHENFELD, D., AND CRUNELLI, V. Low frequency oscillatory activities intrinsic to rat and cat thalamocortical cells. *J. Physiol. Lond.* 441: 155–174, 1991.
- LIVINGSTONE, M. S. AND HUBEL, D. H. Effects of sleep and arousal on the processing of visual information in the cat. *Nature Lond.* 291: 554–561, 1981.
- MADISON, D. V. AND NICOLL, R. A. Control of repetitive discharge of rat CA1 pyramidal neurons in vitro. *J. Physiol. Lond.* 354: 319–331, 1984.
- MCCORMICK, D. A. Functional properties of a slowly inactivating potassium current IAs in guinea pig dorsal lateral geniculate relay neurons. *J. Neurophysiol.* 66: 1176–1189, 1991.
- MCCORMICK, D. A. Cellular mechanisms underlying cholinergic and noradrenergic modulation of neuronal firing mode in the cat and guinea pig dorsal lateral geniculate nucleus. *J. Neurosci.* 12: 278–289, 1992a.
- MCCORMICK, D. A. Neurotransmitter actions in the thalamus and cerebral cortex and their role in neuromodulation of thalamocortical activity. *Prog. Neurobiol.* 39: 337–388, 1992b.
- MCCORMICK, D. A. AND FEESER, H. R. Functional implications of burst firing and single spike activity lateral geniculate relay neurons. *Neuroscience* 39: 103–113, 1990.
- MCCORMICK, D. A., HUGUENARD, H., AND STROWBRIDGE, B. Determination of state dependent processing in thalamus by single neuron properties and neuromodulators. In: *Single Neuron Computation*, edited by T. McKenna, J. Davis, and S. F. Zornetzer. San Diego: Academic, 1992.
- MCCORMICK, D. A. AND PAPE, H.-C. Properties of a hyperpolarization-activated cation current and its role in rhythmic oscillation in thalamic relay neurons. *J. Physiol. Lond.* 431: 291–318, 1990a.
- MCCORMICK, D. A. AND PAPE, H.-C. Noradrenergic and serotonergic modulation of a hyperpolarization-activated cation current in thalamic relay neurons. *J. Physiol. Lond.* 431: 319–342, 1990b.
- MCCORMICK, D. A. AND PRINCE, D. A. Noradrenergic modulation of firing pattern in guinea pig and cat thalamic neurons, in vitro. *J. Neurophysiol.* 59: 978–996, 1988.
- MCMULLEN, T. A. AND LY, N. Model of oscillatory activity in thalamic neurons: role of voltage- and calcium-dependent ionic conductances. *Biol. Cybern.* 58: 243–259, 1988.
- MONTERO, V. M. A quantitative study of synaptic contacts on interneurons and relay cells of the cat lateral geniculate nucleus. *Exp. Brain Res.* 86: 257–270, 1991.
- PAPE, H. C. Adenosine promotes burst firing activity in guinea pig geniculocortical neurons through two different mechanisms. *J. Physiol. Lond.* 447: 729–753, 1992.
- PENNEFATHER, P., LANCASTER, B., ADAMS, P. R., AND NICOLL, R. A. Two distinct Ca-dependent K currents in bullfrog sympathetic ganglion cells. *Proc. Natl. Acad. Sci. USA* 82: 3040–3044, 1985.
- ROSE, R. M. AND HINDMARSH, J. L. A model of a thalamic neuron. *Proc. R. Soc. Lond. B Biol. Sci.* 225: 161–193, 1985.
- ROSE, R. M. AND HINDMARSH, J. L. The assembly of ionic currents in a thalamic neuron. I–III. *Proc. R. Soc. Lond. B Biol. Sci.* 237: 267–334, 1989.
- RUDY, B. Diversity and ubiquity of K channels. *Neuroscience* 25: 729–749, 1988.
- SHERMAN, S. M. AND KOCH, C. The control of retinogeniculate transmission in the mammalian lateral geniculate nucleus. *Exp. Brain Res.* 63: 1–20, 1986.
- SOLTESZ, I., LIGHTOWLER, S., LERESCHE, N., JASSIK-GERSCHENFELD, D., POLLARD, C. E., AND CRUNELLI, V. Two inward currents and the transformation of low frequency oscillations of rat and cat thalamocortical cells. *J. Physiol. Lond.* 441: 175–197, 1991.
- STERIADE, M., CURRÓ DOSSI, R., AND NUNEZ, A. Network modulation of a slow intrinsic oscillation of cat thalamocortical neurons implicated in sleep delta waves: cortical potentiation and brainstem suppression. *J. Neurosci.* 11: 3200–3217, 1991.
- STERIADE, M. AND DESCHÊNES, M. The thalamus as a neuronal oscillator. *Brain Res. Rev.* 8: 1–63, 1984.
- STERIADE, M. AND LLINÁS, R. R. The functional states of the thalamus and the associated neuronal interplay. *Physiol. Rev.* 68: 649–742, 1988.
- STERIADE, M. AND MCCARLEY, R. W. *Brainstem Control of Wakefulness and Sleep*. New York: Plenum, 1990.
- STORM, J. F. Action potential repolarization and a fast after-hyperpolarization in rat hippocampal pyramidal cells. *J. Physiol. Lond.* 385: 733–759, 1987.
- STORM, J. F. Potassium currents in hippocampal pyramidal cells. *Prog. Brain Res.* 83: 161–187, 1990.
- TRAUB, R. D., WONG, R. K. S., MILES, R., AND MICHELSON, H. A model of a CA3 hippocampal pyramidal neuron incorporating voltage-clamp data on intrinsic conductances. *J. Neurophysiol.* 66: 635–650, 1991.
- YAMADA, W. M., KOCH, C., AND ADAMS, P. Multiple channels and calcium dynamics. In: *Methods in Neuronal Modeling. From Synapses to Networks*, edited by C. Koch and I. Segev. Cambridge, MA: MIT Press, 1989, p. 97–133.
- WANG, X.-J., RINZEL, J., AND ROGAWSKI, M. A. A model of the T-type calcium current and the low threshold spike in thalamic neurons. *J. Neurophysiol.* 66: 839–850, 1991.
- WESTENBROEK, R. E., AHLJANIAN, M. K., AND CATTERALL, W. A. Clustering of L-type Ca<sup>2+</sup> channels at the base of major dendrites in hippocampal pyramidal neurons. *Nature Lond.* 347: 281–284, 1990.